

Journal Pre-proof

Coccolithophore export in three deep-sea sites of the Aegean and Ionian Seas (Eastern Mediterranean): Biogeographical patterns and biogenic carbonate fluxes

E. Skampa, M.V. Triantaphyllou, M.D. Dimiza, A. Gogou, E. Malinverno, S. Stavrakakis, C. Parinos, I.P. Panagiotopoulos, D. Tselenti, O. Archontikis, K.-H. Baumann

PII: S0967-0645(19)30041-4

DOI: <https://doi.org/10.1016/j.dsr2.2019.104690>

Reference: DSR II 104690

To appear in: *Deep-Sea Research Part II*

Received Date: 31 January 2019

Revised Date: 10 November 2019

Accepted Date: 14 November 2019

Please cite this article as: Skampa, E., Triantaphyllou, M.V., Dimiza, M.D., Gogou, A., Malinverno, E., Stavrakakis, S., Parinos, C., Panagiotopoulos, I.P., Tselenti, D., Archontikis, O., Baumann, K.-H., Coccolithophore export in three deep-sea sites of the Aegean and Ionian Seas (Eastern Mediterranean): Biogeographical patterns and biogenic carbonate fluxes, *Deep-Sea Research Part II* (2019), doi: <https://doi.org/10.1016/j.dsr2.2019.104690>.

This is a PDF file of an article that has undergone enhancements after acceptance, such as the addition of a cover page and metadata, and formatting for readability, but it is not yet the definitive version of record. This version will undergo additional copyediting, typesetting and review before it is published in its final form, but we are providing this version to give early visibility of the article. Please note that, during the production process, errors may be discovered which could affect the content, and all legal disclaimers that apply to the journal pertain.

© 2019 Published by Elsevier Ltd.



Coccolithophore export in three deep-sea sites of the Aegean and Ionian Seas (Eastern Mediterranean): biogeographical patterns and biogenic carbonate fluxes

E. Skampa¹, M.V. Triantaphyllou¹, M.D. Dimiza¹, A. Gogou², E. Malinverno³, S. Stavrakakis², C. Parinos², I.P. Panagiotopoulos^{1,2}, D. Tselenti¹, O. Archontikis¹, K.-H. Baumann⁴

¹National and Kapodistrian University of Athens, Faculty of Geology and Geoenvironment, Panepistimioupolis, 15784 Athens, Greece

²Hellenic Centre for Marine Research, Institute of Oceanography, PO Box 712, 19013 Anavyssos, Greece

³University of Milano-Bicocca, Department of Earth and Environmental Sciences, Italy

⁴University of Bremen, Department of Geosciences, PO Box 33 04 40, 28334 Bremen, Germany

Abstract

Coccolithophore export fluxes were investigated via the analysis of sinking matter, obtained from Eastern Mediterranean time-series sediment traps moored in three open sites of the north-eastern Mediterranean Sea located in the Athos Basin of North Aegean (M2 site), Cretan Sea of South Aegean (M3 site) and at Ionian Sea (Nestor site). The aim of our study was to determine the spatial, temporal and seasonal variability in coccolithophore fluxes, as well as to estimate coccolith biogenic carbonate contribution to the sedimentation process. Data from an additional time-series sediment trap located in the southwestern Black Sea were also considered for the comparison of the oligotrophic Eastern Mediterranean setting with the eutrophic Black Sea. Coccolithophore fluxes revealed a highly seasonal pattern during February-March in the North Aegean (peak in late February 2015: 85.6×10^5 coccospheres $\text{m}^{-2} \text{day}^{-1}$; 27.9×10^8 coccoliths $\text{m}^{-2} \text{day}^{-1}$), during March-May in the Cretan Sea (peak in late March 2015: 33.7×10^5 coccospheres $\text{m}^{-2} \text{day}^{-1}$; 19.5×10^8 coccoliths $\text{m}^{-2} \text{day}^{-1}$) and during February-March and May-June in the Ionian Sea (peak in late May 2012: 14.3×10^5 coccospheres $\text{m}^{-2} \text{day}^{-1}$; 1.53×10^8 coccoliths $\text{m}^{-2} \text{day}^{-1}$). The recorded maxima coincide with low sea surface temperatures, increased precipitation and high PIC fluxes. Coccosphere fluxes were dominated by *Emiliana huxleyi* comprising ~70% of the total abundance, in the North Aegean and ~50% in the Cretan and Ionian Seas. *Syracosphaera pulchra* was also prominent in the study sites, where its abundance reached 14% in the North Aegean and ~10% in the Cretan and Ionian Seas respectively. *Florisphaera profunda* represented one of the major taxa in the coccolith fluxes of all three Eastern Mediterranean sites (~25% in North Aegean, ~20% in Cretan and Ionian Seas), while *Algirosphaera robusta* and *Umbilicosphaera sibogae* were the most abundant among the minor taxa. The North Aegean Sea exhibited a considerably higher coccolith flux when compared to other sediment traps due to the prominent seasonal peak of *E. huxleyi* during winter (February-March) (>95% of the total abundance). In contrast to the Eastern Mediterranean sediment traps, the time-series data from the

Black Sea showed presence of monospecific *E. huxleyi* assemblage increasing its abundance during late September-November (max 320×10^5 coccospheres $\text{m}^{-2} \text{day}^{-1}$; at least 7.79×10^8 coccoliths $\text{m}^{-2} \text{day}^{-1}$, coccolith flux derived only from coccospheres converted to coccoliths). In the Eastern Mediterranean, biogenic carbonate fluxes followed the general pattern of the total mass flux in all investigated areas, with the Black Sea coccolithophore CaCO_3 flux being the lowest due to low the *E. huxleyi* coccolith mass. Overall, in the North Aegean Sea, coccolithophore fluxes are strongly dependent on surface waters nutrients enrichment due to winter vertical water column mixing, riverine inputs and Black Sea water inflows, while the fertilization and/or formation of fast-sinking aggregates due to episodic dust input event are affecting the coccolithophore fluxes in the Cretan and Ionian Seas. The intercomparison of the coccolith export fluxes in the studied NE-SW mooring transects implies a north-south and east-west decreasing pattern, depending on the variable oceanographic regimes and the associated environmental factors controlling the investigated areas.

Keywords: coccolithophores; Eastern Mediterranean; Black Sea; sediment trap time-series; seasonal productivity

1. Introduction

Coccolithophores are marine photosynthetic unicellular organisms, comprising an important role in the CO_2 - O_2 exchange between the oceans and the atmosphere. They impact both the biological and carbonate pumps (Rost and Riebsell, 2004) and have an ability to modify upper-ocean alkalinity. CO_2 is released during coccolith formation, while part of the photosynthetically fixed CO_2 is redistributed into the deep ocean and the seafloor (Westbroek et al., 1993; Le Moigne, 2019). Coccolithophores contribute significantly to particulate inorganic carbon (PIC), representing a major part of the calcium carbonate mineral produced in the surface that sinks in the deep waters, and gets stored in sediments, fuelling the carbonate pump (Westbroek et al., 1993). The group is usually related to oligotrophic conditions in low and middle latitude regions (e.g. McIntyre and Bé, 1967; Winter et al., 1994; Ziveri et al., 2004). However, their productivity is regionally affected by local phenomena such as coastal currents, gyres, eddies, upwelling and river runoffs (Cachão and Moita, 2000; Ziveri et al., 2004). Coccolithophores represent one of the major planktonic groups that despite their strong seasonal variability, contribute significantly to the biogenic carbonate export flux in the Eastern Mediterranean Sea (Knappertsbusch, 1993; Ziveri et al., 1995, 2000a, b; Malinverno et al., 2003, 2009, 2014; Triantaphyllou et al., 2004).

In the oligotrophic waters of the Eastern Mediterranean Sea, seasonal variations in solar radiation, sea surface temperatures (SSTs), nutrient concentrations and the circulation of surface water masses affect coccolithophore abundance and productivity, nevertheless resulting in high taxa number that are strongly linked to seasonal variability (Kleijne, 1991; Triantaphyllou et al., 2002, 2015; Malinverno et

al., 2003; Ignatiades et al., 2009; Dimiza et al., 2008, 2015). Previous sediment trap studies in the Eastern Mediterranean Sea (e.g. Ziveri et al., 2000b, Triantaphyllou et al., 2004, 2014, Malinverno et al., 2009; 2014) have revealed seasonal fluctuation in primary productivity related to annual variations in the SST and precipitation. Productivity maxima are recorded during the late winter to spring, causing a different ascendancy of taxa and a shift in the vertical water column. All previous studies have reported *Emiliania huxleyi* as the dominant species in the upper photic zone (UPZ) and *Florisphaera profunda* as the dominant species in the lower photic zone (LPZ).

Time-series sediment traps are one of the few available tools for monitoring particle export fluxes over extended periods of time (Forbes et al., 1992; Gislason and Asithorsson, 1992, Rigual-Hernández et al., 2015; Danovaro et al., 2017), which have been shown to contribute to global oceanic calcium carbonate budgets (Broerse et al., 2000a, b). Time-series of settling coccolithophores collected by sediment traps provide a good alternative for assessing the seasonal variation of marine phytoplankton and the relative proportion of individual species or taxa in the pelagic marine environment (e.g. Milliman, 1993; Baumann et al., 2005; Guerreiro et al., 2017). Coccolithophore fluxes not only reflect the overlying production but sinking mechanisms as well (Broerse et al., 2000c). Plenty of individual coccoliths, shed by coccospheres, are suspended in the euphotic layer; the latter are grazed by zooplankton (e.g., copepods) forming faecal pellets and sink as macro-aggregates to the seafloor (e.g., Honjo, 1976; Nowald et al., 2006). The sinking speed of such densely-packed pellets is relatively high (as much as 570 m day^{-1} ; Fischer and Karakas, 2009) and potentially triggered by phytoplankton blooms (e.g., Nowald et al., 2006), while individual coccospheres in the Eastern Mediterranean Sea sink with a rate of approximately 100 m day^{-1} (Ziveri et al., 2000b). Coccolith deposition on the seafloor mainly occurs via the sinking of faecal pellets, as the small number of individual sinking coccoliths is affected by dissolution processes (Honjo, 1976). Yet, more information is needed to develop a better understanding of the way that seasonal environmental processes affect the extant coccolithophore ecological signal that gets transferred to the ocean bottom as sinking flux and eventually becomes imprinted in the underlying deep-sea sediments (Baumann et al., 2005; Malinverno et al., 2014; Meier et al., 2014).

In the present study, coccolithophore export flux has been investigated in sediment traps samples collected during various time intervals from three Eastern Mediterranean sites (Fig. 1; Tables 1, 2): the mesotrophic North Aegean Sea (Athos Basin, M2 site; January-December 2011, October 2014-November 2015), the ultra-oligotrophic Cretan Sea/South Aegean (M3 site; January 2001-February 2002, January-December 2015) and the oligotrophic Ionian Sea (Nestor site; January 2011-August 2012, October 2014-September 2015). The obtained results were compared with coccolithophore export flux dataset from the western Black Sea (Fig. 1) to document differences in coccolithophore export flux between the eutrophic Black Sea and the oligotrophic Eastern Mediterranean Sea. The studied sediment traps data sets will be helpful to define spatial, temporal and seasonal variability in

coccolithophore fluxes and assemblage composition and the acquired information will enable understanding of the various mechanisms that control the water column biogenic sedimentation in the Eastern Mediterranean Sea.

2. Oceanographic Settings

The hydrology of the Aegean and Ionian Seas features complex water mass dynamics with cyclonic and anticyclonic eddies defining the water mass distribution. Specific identification criteria of the various basins hydrological regimes are presented in Table 3.

2.1. North Aegean Sea

The North Aegean Sea bears a complicated physical and geographic configuration, as it is connected in the northeast with the Black Sea through the Dardanelles Straits and Marmara Seas. Low-saline (24–28 psu) surface (<70 m depth) Black Sea Water (BSW) flows through the Dardanelles straits along the eastern coast of Greece until it reaches the southwestern Aegean Sea (Lykousis et al., 2002) (Table 3). BSW inflow rates are featured by seasonal and interannual variability, with maximum values during the mid to late summer (July-August) and lowest during the winter (December-February) (Zervakis et al., 2000, 2004). Warm and salty (>39 psu) Levantine Surface Water (LSW) is present when BSW is absent, whereas Levantine Intermediate Water (LIW; 14–15°C, 38.8–39.1 psu) extends to a depth of about 400 m below the BSW/LSW. The inflow of the BSW mass causes enrichment in particulate and dissolved organic matter, leading to enhanced planktonic biomass and primary production (e.g., Ignatiades et al., 2002; Lagaria et al., 2013; Karatsolis et al., 2016; Skampa et al., 2019).

Although the North Aegean Sea displays overall oligotrophic characteristics, seasonal mesotrophic features are present during the high-productivity spring period, under the influence of the BSW inflow, with Chl-a reaching concentration of $1 \mu\text{g L}^{-1}$ (Ignatiades et al., 2002; Zervoudaki et al., 2011; Lagaria et al., 2013; Malinverno et al., 2016). The Deep Chlorophyll Maximum (DCM) located within the LSW mass at around 60m depth (Lagaria et al., 2013). Surface Chl-a concentrations derived from satellite measurements for the studied period, ranged from 0.1 to $1.31 \mu\text{g L}^{-1}$, following a seasonal pattern. High values are found during late fall-winter (November-February), with maxima from late winter to early spring (February-April) (Supplementary Fig. 1). The sea surface productivity cycle is opposite to that of the SST (Supplementary Fig. 1), which subdivides the annual cycle in to the warm (May-October) and a cold season (November-April) (values up to 27.9°C and 19.3°C respectively). The SST pattern is anticorrelated with the annual variation of precipitation (Supplementary Fig. 1; peak during fall 2014-winter 2015). Precipitation and riverine-driven nutrient inputs, especially during winter time, supply the North Aegean Basin with land-derived organic matter, enhancing marine productivity (Poulos et al., 1997; Roussakis et al., 2004; Skampa et al., 2019).

2.2. Cretan Sea

The Cretan Sea (Fig. 1) comprises the largest and deepest basin (2500 m depth) of the South Aegean Sea and is connected to both Levantine Basin (east) and Ionian Sea (west) through the Antikythira and Kassos Straits respectively. The Cretan Sea receives most of the saline waters from the Levantine Basin and less from the North Aegean Sea (Theocharis et al., 1986; Lascaratos and Papageorgiou, 1987) and acts as reservoir for dissolved oxygen, salt and heat that causes a net loss of water to the atmosphere (Georgopoulos et al., 1989, 2000). The warm and saline LSW (>39.3 psu) and the low salinity Modified Atlantic Water (MAW), mostly traced as a surface/subsurface salinity minimum (~ 38.5 – 38.9 psu; Velaoras et al., 2014), represent the most important water masses of the Cretan Sea upper water column (Table 3). The warmer and saline Levantine Intermediate Water mass (LIW) ($38.9 < S < 39.1$ psu; Velaoras et al., 2014) is located in the intermediate layers of the water column, while the oxygenated Cretan Deep Water (CDW) with $S \sim 39.08$ psu occurs in the deep layers (Table 3).

The persistence of low concentrations of nutrients, low primary productivity values and phytoplankton densities characterize the ultra-oligotrophic Cretan Sea waters with the formation of pronounced DCM (at 75–100m depth) throughout most of the year (Psarra et al. 2000; Tselepides et al. 2000). Surface Chl-a concentrations, as derived from satellite measurements for the studied time period (Supplementary Fig. 1), present maximum values during winter-early spring, i.e. during SST minima and precipitation maxima, with highest peak in late February 2015 ($0.23 \mu\text{g L}^{-1}$). The SST values (Supplementary Fig. 1) subdivide the annual cycle in a warm (May–October) and a cold season (November–April), ranging seasonally from 15.5°C to 27.9°C with maxima during late August 2010. The opposite pattern characterises the annual variation of precipitation, with the rainy season occurring during fall-early spring, peaking in early December 2010 (Supplementary Fig. 1).

2.3. Ionian Sea

The submarine morphology of the Ionian Sea is complicated with steep slopes, valleys and deep basins, which incorporate the deepest basins of the Mediterranean Sea (4600 and 5264 m depth; e.g., Stavrakakis et al., 2013). The structure of the local water masses (Table 3) consists of the MAW (upper 25–100 m), which is characterized by a salinity minimum (average Temperature= 17.4°C and Salinity= 38.72 psu), the LIW (100–500 m) showing a salinity maximum, the Transitional Waters (TW; layer between 500 and 1200 m; average Temperature= 13.8°C and Salinity= 38.76 psu) and the Eastern Mediterranean Deep Waters (EMDW: layers below 1200 m; average Temperature= 13°C and Salinity= 38.6 psu) (Nittis et al., 1993; Malanotte-Rizzoli et al., 1997). In open areas of the Ionian Sea, surface Chl-a concentrations are generally lower than 0.5 mg L^{-1} with the DCM located at 80–100 m depth (e.g., Crombet et al., 2011; Karageorgis et al., 2012). That makes the Ionian Sea, a highly oligotrophic region (Boldrin et al., 2002; Malinverno et al., 2003; Ignatiades, 2005); subsequently, on-

going oligotrophic conditions result in low seasonality (Casotti et al., 2003). Surface Chl-a concentrations as derived from satellite measurements for the studied time interval (Supplementary Fig. 1) display a seasonal pattern with the highest values occurring during late winter-spring (max: April 2012; $0.29 \mu\text{g L}^{-1}$; Fig. Supplementary Fig. 1) SST values subdividing the annual cycle in a warm (May-October) and a cold season (November-April), range from 15.1°C to 29.3°C . An anti-correlated pattern is followed by the precipitation with the rainy season maxima occurring during late winter-spring.

2.4. Black Sea

The Black Sea is world's largest semi-enclosed marginal sea, with a maximum depth of more than 2200 m (Ross and Degens, 1974). The narrow and shallow Bosphorus and Dardanelles Straits provide the only pathways of water exchange between the Black Sea and the northeastern Mediterranean. The Black Sea is impacted by the discharges of major rivers (e.g., Danube, Dniester etc.; Leppäkoski and Mihnea, 1996), therefore acquiring salinities equivalent to brackish environments with values of 17 psu in the surface waters near Bosphorus Straits and 22.3 psu in the Deep Water layer of the Black Sea (Talley et al., 2011). The inflow of nutrients via riverine discharge combined with the frequent upwelling of nutrient rich waters supports the establishment of a highly productive ecosystem (Sorokin, 1983; Hay et al., 1990; Humborg et al., 1997; Cokacar et al., 2004).

The surface circulation of the Black Sea presents a cyclonic gyre, known as the Rim Current, that roughly follows the continental shelf break, including a series of anticyclonic eddies or small gyres (Oguz et al., 1993; Talley et al., 2011). The hydrological balance results in prominent water column stratification and an absence of dissolved oxygen below the pycnocline (Oguz et al., 1993; 2006; Korotaev et al., 2003). The upper low salinity, oxygenated (oxic) waters are featured by a thin subsurface chlorophyll maximum (<20 m thickness, centred around 40 m depth; Oguz et al., 1999) and are separated with a sharp halocline (between 50–100 m depth) from the deeper oxygen-free (anoxic) layers (Talley et al., 2011). The Cold Intermediate Layer, most likely a remnant of the winter surface mixed layer, has a subsurface temperature minimum of $<8^{\circ}\text{C}$ near 100 m depth, and overlies the Deep Water that has a salinity of 22.3 psu and temperature of 8.9°C (Talley et al., 2011). Within the investigated time interval (October 2007-September 2008) Chl-a concentrations ranged from 0.58 to $1.1 \mu\text{g L}^{-1}$ (Talley et al., 2011) with highest values documented during late fall 2007 (October-November; Supplementary Fig. 1). Precipitation displayed a similar pattern, showing higher values in fall (119 mm in November 2007) and late spring (80 mm in April 2008) (Supplementary Fig. 1). During the investigated period (October 2007-September 2008), SST values in the study area ranged from 7.8°C to 23.6°C based on satellite datasets dividing the annual cycle in a warm (April-October) and a cold (November-March) period.

3. Material and methods

Three PPS3/3 Technicap sediment traps (0.125 m² collecting area, 12 receiving cups, with individual sampling intervals of ~15 days.; Table 1) were deployed at different sites of the Eastern Mediterranean Sea (127 samples in total; for details see Fig.1 and Table 2) during various time intervals. Two deployments were moored in the Aegean Sea; in the North Aegean Sea (Athos Basin, M2 site; 39° 58.16'N, 24°43.48'E) at 500 m depth (June 2011-November 2015, missing the interval January 2012-September 2014) and in the Cretan Sea (35°44.76'N, 25°09.29'E) at 500 m (February 2001-January 2002) and 1500 m depth (January 2015-December 2015). A third mooring was deployed in the south Eastern Ionian Sea (Nestor site; 36°2.96'N, 21°28.93'E; June 2010-September 2015; missing the interval September 2012-September 2014) at 2000 m. An previously published site from the southwestern Black Sea (42°58.00'N, 29°29.00'E) at 965m depth (October 2007-September 2008; Bouloubassi et al., 2010) has been considered in order to compare the oligotrophic Eastern Mediterranean Sea time series with a eutrophic and less saline setting.

The recovered trap samples were kept in the dark at 4°C, until treated in the laboratory. An 1mm nylon sieve was used in a part of the supernatant, to remove large organisms, whereas, smaller than 1mm swimmers were removed by hand, under a light microscope using fine tweezers. Each sample was divided into subsamples by a high-precision peristaltic, microprocessor-controlled dispensing pump.

Total mass fluxes (Figs. 2a-d) were calculated from the dry weights of the subsamples used for opal analyses, following Stavrakakis et al. (2000) and Stavrakakis et al. (2013). For the determination of organic carbon (OC), subsamples of 8mg of sinking matter, were filtered through pre-combusted (450°C), pre-weighed GF/F filters which then were stored at ~20°C in the dark, until analysis. OC contents were measured with a Thermo Scientific FLASH 2000 CHNS elemental analyzer in HCl treated and non-treated samples, respectively (Nieuwenhuize et al., 1994). The calculation of particulate inorganic carbon (PIC) components was carried out by subtracting the organic carbon from the total carbon measured, assuming all inorganic carbon was CaCO₃ and using the molecular mass ratio 100/12 [(TC%-OC%)×8.33] (e.g., Stavrakakis et al., 2013). The estimation of lithogenic fraction (quartz, aluminosilicates, heavy minerals etc.) was calculated by subtraction of the sum of biogenic components from 100 [lithogenic% = 100% -(organic matter%+carbonates%+opal%)] (Stavrakakis et al., 2013).

Each subsample used for coccolithophore analysis was first split into 10 equal fractions by the use of McLane rotary wet splitter, with less than 4% deviation between aliquots. A vacuum pump was used to filter the produced aliquots onto Millipore cellulose filters (47 mm diameter, 0.45 µm pore size). The splitting was processed using buffered distilled water (pH>8); filters were dried in oven and stored in plastic petri dishes. For coccolith sample preparation aliquots were further split into 10 equal

fractions; organic material was oxidized following Bairbakhish et al. (1999) and each sub-sample was sieved over a 32 μm mesh sieve. For each sample, two slides were prepared by mounting approximately 30 mm^2 of filter from coccosphere and coccolith splits respectively, and were analysed using a polarized light optical Leica DMLSP microscope (LM) at 1250x.

Approximately 20 mm^2 area was investigated to determine total coccosphere fluxes and coccospheres per taxa (an average number of approximately 50 cells per sample), whereas total coccoliths and coccoliths per species were counted within an area of 2 mm^2 (approximately 600 coccoliths were counted on average per sample) (e.g., Ziveri et al., 2000b; Triantaphyllou et al., 2004). Coccolithophore fluxes were calculated via extrapolation to the entire effective filtration area and total sample, according to the following equation (Ziveri et al., 1999):

$$F = N \times A_f \times S / a_f \times A_{st} \times T,$$

Where,

F=flux ($\text{specimens m}^{-2}\text{day}^{-1}$),

N=number of counted specimens,

A_f =effective filtration area (mm^2),

S=split factor,

a_f =investigated filtration area (mm^2),

A_{st} =sediment-trap aperture area (m^2),

T=sample collecting time (days).

Coccosphere units were converted to coccolith numbers using the mean number of coccoliths per coccosphere per species (Table 4), following the approach of Boeckel and Baumann (2008). Average relative abundances were estimated by calculating the average relative abundance of each taxon in all samples at all sites, during all investigated time intervals. The coccolith carbonate fluxes were calculated by using estimates of the carbonate mass per coccolith for the individual coccolith taxa and size calibrations for reliable results (Young and Ziveri, 2000; Baumann, 2004). Since total carbonate and coccolithophore carbonate fluxes were estimated differently, deviations may occur due to methods analytical limits.

Coccolith mass for *Emiliania huxleyi* was calculated according to the equation of Young and Ziveri (2000), based on estimations of morphometrical analysis from Scanning Electron Microscope (SEM) images, in order to achieve accurate coccolith mass results. For the morphometric analyses on *E. huxleyi* coccoliths, a piece of a filter was attached to a copper stub of 1 cm diameter using a double sided adhesive tape and coated with gold for 2 minutes. Each sample was scanned under JEOL JSM

6360 SEM and 40 flat-lying *E. huxleyi* coccoliths in the distal view (in total 1807 coccoliths) were captured at 10,000 \times magnification. The morphometric analysis of coccolith (Supplementary Appendix 1) was carried out using ImageJ software, following the macro routines of Young et al. (2014). The measured coccolith size parameters were then applied to the equation of Young and Ziveri (2000) for the calculation of coccolith mass (see Table 5). For coccosphere carbonate weights *Emiliania huxleyi*, *Syracosphaera pulchra*, *Algirosphaera robusta*, *Umbilicosphaera sibogae* were included in the coccolith mass by using the mean number of coccoliths per coccosphere per taxa (Boeckel and Baumann, 2008) (Table 5).

Spearman's correlation coefficient (r) analysis was carried out to determine relationships between total coccolithophore and major taxa fluxes with the rest physico-chemical components of the flux provided from the four investigated sediment traps (Table 6). All statistical analyses were performed using SPSS (version 10.1) statistical software.

All satellite data (Chl-a, Precipitation, Sea Surface Temperature; Supplementary Fig. 1a-d) were obtained from <http://disc.sci.gsfc.nasa.gov/giovanni/> (Acker and Leptoukh, 2007); An average of 8 days data for satellite chlorophyll a (Chl-a) concentration from MODIS-Aqua (MODerate resolution imaging spectroradiometer) 4 km resolution for the following boxes was obtained from the National Aeronautic and Space Administration (NASA) Giovanni website (<http://disc.sci.gsfc.nasa.gov/techlab/giovanni/>). The coordinates of satellite data obtained were, 1) North Aegean Sea: Chl-a, SST: 39.9375-40.0625 °N, 24.4375-24.5625 °E, precipitation: 39.875-39.875 °N, 24.375-24.375 °E; 2) Cretan Sea: Chl-a, SST: 35.5208-35.8958 °N, 24.9792-25.3125 °E, precipitation: 35.625-35.875 °N, 25.125-25.125 °E; 3) Ionian Sea: Chl-a, SST: 36.2292-36.5625°N, 21.2292-21.5625 °E, precipitation: 36.375-36.375 °N, 21.375-21.375 °E

4. Results

4.1. Correlations

Total coccolithophore flux and *E. huxleyi* and *Florisphaera profunda* fluxes in all investigated sites were positively correlated within a 0.01 level of significance when applying the Spearman's correlation coefficient to the major components of the flux (total mass, carbonate, lithogenics, total organic carbon and PIC fluxes; Table 6).

4.2. North Aegean Sea

The highest value of total mass flux for the entire sampled period was reached during late October 2014 (2272 mg m⁻² day⁻¹; Fig. 2a). Similar to the total mass flux, total carbonate (142.83 mg m⁻² day⁻¹), total organic carbon (38.33 mg m⁻² day⁻¹) and total coccolithophore carbonate fluxes (96.09 mg m⁻² day⁻¹) show higher values during the low SST interval (12.4–14.5°C) of winter and early spring 2015 (Fig. 2a). The lithogenic flux (up to 70% of the total mass flux) followed the general pattern with

maximum ($576\text{--}820\text{ mg m}^{-2}\text{ day}^{-1}$) appearance during winter-early spring 2015 (February-March) and the highest peak during early January 2015 ($820\text{ mg m}^{-2}\text{ day}^{-1}$), which positively correlated with the precipitation peak (Fig. 2a). PIC flux (up to 3.3% of the total mass flux) fluctuated similarly to the lithogenic flux, with maxima occurring during winter 2015 (February: $17.15\text{ mg m}^{-2}\text{ day}^{-1}$; Fig. 2a)

Total coccolithophore fluxes in the North Aegean Sea (late January-December 2011, Triantaphyllou et al., 2014; late October 2014-early November 2015, present study) displayed maxima during late winter-early spring (February-March 2015), with a prominent peak in late February 2015 (85.6×10^5 coccospheres $\text{m}^{-2}\text{ day}^{-1}$; 27.9×10^8 coccoliths $\text{m}^{-2}\text{ day}^{-1}$; Fig. 3a) (Supplementary Appendix 2). Coccosphere fluxes presented much lower values in the available 2011 dataset, with the highest values reaching 2.91×10^5 coccospheres $\text{m}^{-2}\text{ day}^{-1}$ in early December (Fig. 3a).

Emiliania huxleyi dominated during the whole investigated time interval, following the general trend of the total coccolithophore export flux. During 2011, two major peaks of this species occurred during late June and early December (2.38×10^5 coccospheres $\text{m}^{-2}\text{ day}^{-1}$ and 2.22×10^5 coccospheres $\text{m}^{-2}\text{ day}^{-1}$, respectively; Fig. 3a). Although there is no available coccosphere data for the first semester of 2011, the coccolith flux of the species suggests a major peak in February 2011 (12.7×10^8 coccoliths $\text{m}^{-2}\text{ day}^{-1}$). Highest numbers of *E. huxleyi* were recorded during February and March (maximum flux in late February 2015: 79.2×10^5 coccospheres $\text{m}^{-2}\text{ day}^{-1}$; 16.1×10^8 coccoliths $\text{m}^{-2}\text{ day}^{-1}$; Fig. 3a). Taxa that also contributed to the total coccolithophore flux of the North Aegean Sea were *F. profunda* and *S. pulchra* followed by *A. robusta* and *U. sibogae* (Supplementary Appendix 2). A higher relative abundance of *F. profunda* and *S. pulchra* was observed during the warm period (May-October), coupled with *E. huxleyi* minima. Highest fluxes of *F. profunda* were recorded during late February (2011: 4×10^8 coccoliths $\text{m}^{-2}\text{ day}^{-1}$; 2015: 10.4×10^8 coccoliths $\text{m}^{-2}\text{ day}^{-1}$, Fig. 3a) and early June (2011: 4.35×10^8 coccoliths $\text{m}^{-2}\text{ day}^{-1}$; 2015: 5.65×10^8 coccoliths $\text{m}^{-2}\text{ day}^{-1}$, Fig. 3a). *Syracosphaera pulchra* displayed very low coccosphere and coccolith fluxs within 2011 (up to 0.14×10^5 coccospheres $\text{m}^{-2}\text{ day}^{-1}$; 0.07×10^8 coccoliths $\text{m}^{-2}\text{ day}^{-1}$; Fig. 3a). In contrast, *S. pulchra* maximum coccosphere flux has been recorded in early June 2015 (up to 3.36×10^5 coccospheres $\text{m}^{-2}\text{ day}^{-1}$; Fig. 3a) and maximum coccolith flux in late December (1.24×10^8 coccoliths $\text{m}^{-2}\text{ day}^{-1}$; Fig. 3a). The large coccolith-bearing taxa *Helicosphaera carteri* and *Pontosphaera* spp. displayed relative abundances < 1%, contributing to the flux with values up to 0.32×10^5 coccospheres $\text{m}^{-2}\text{ day}^{-1}$, 0.12×10^8 coccoliths $\text{m}^{-2}\text{ day}^{-1}$ and 0.02×10^8 coccoliths $\text{m}^{-2}\text{ day}^{-1}$ respectively; with the latter taxon presented only in coccolith fluxes (Supplementary Appendix 2). Other taxa such as *Syracosphaera mediterranea* (ex. *Coronosphaera mediterranea*; Triantaphyllou et al., 2015), *Calcidiscus leptoporus*, *Calciosolenia* spp., *Umbellosphaera tenuis*, *Rhabdosphaera clavigera* and *Discosphaera tubifera* were practically negligible as they contributed to the assemblages very sporadically and with abundances of <1%. Total minor taxa coccolith flux (also including coccospheres converted to coccolith units) exhibited highest peak during early August 2015 (1.39×10^8 coccoliths $\text{m}^{-2}\text{ day}^{-1}$; Fig. 3b).

4.3. Cretan Sea

The observed pattern of total mass flux in the Cretan Sea was characterised by high peaks during the spring period, with maxima during late March 2015 ($496 \text{ mg m}^{-2} \text{ day}^{-1}$; Fig. 2b) followed by April 2001 and April 2015 (425.39 and $305.95 \text{ mg m}^{-2} \text{ day}^{-1}$ respectively; Fig. 2b), and moderate values for the rest of the year ($29.21\text{--}170 \text{ mg m}^{-2} \text{ day}^{-1}$; Fig. 2b). The same seasonal maxima was recorded by the total carbonate ($210 \text{ mg m}^{-2} \text{ day}^{-1}$), total organic carbon ($14 \text{ mg m}^{-2} \text{ day}^{-1}$) and total coccolithophore carbonate fluxes ($137.92 \text{ mg m}^{-2} \text{ day}^{-1}$) (Fig. 2b). The lithogenic flux, which was less than 55% of the total mass flux, followed the same pattern as well, with maximum values appearing in March 2015 ($820 \text{ mg m}^{-2} \text{ day}^{-1}$; Fig. 2b). PIC (max. 5% of the total mass flux) matched with the lithogenic flux, with maxima occurring in March 2015 ($25.2 \text{ mg m}^{-2} \text{ day}^{-1}$; Fig. 2b).

Total coccolithophore fluxes in the Cretan Sea (January 2001–February 2002, 500 m depth, Triantaphyllou et al., 2004; January 2015–December 2015, 1550m depth, present study) displayed a seasonal pattern with major increase recorded in the late winter-early spring 2015 (February to March: $1.14 \times 10^5\text{--}33.7 \times 10^5$ coccospheres $\text{m}^{-2} \text{ day}^{-1}$; $2.59 \times 10^8\text{--}19.5 \times 10^8$ coccoliths $\text{m}^{-2} \text{ day}^{-1}$; Fig. 4a) (Supplementary Appendix 2). Although the total coccolithophore export fluxes of 2015 were generally lower than those of the annual cycle 2001–2002, coccosphere and coccolith flux peaks recorded in late March 2015 (maximum flux: 33.7×10^5 coccospheres $\text{m}^{-2} \text{ day}^{-1}$; 19.5×10^8 coccoliths $\text{m}^{-2} \text{ day}^{-1}$; Fig. 5a) were considerably higher than the values of 2001 (early April 2001: 3.97×10^5 coccospheres $\text{m}^{-2} \text{ day}^{-1}$; 9×10^8 coccoliths $\text{m}^{-2} \text{ day}^{-1}$; Fig. 4a).

During the study, *E. huxleyi* was the dominant species of the assemblage following the total coccolithophore export flux pattern. *Emiliania huxleyi* coccolith flux fluctuations tracked the species coccosphere flux with maxima displayed during early spring. The highest values occurred during late March 2015 (max. 13.1×10^5 coccospheres $\text{m}^{-2} \text{ day}^{-1}$; 13.38×10^8 coccoliths $\text{m}^{-2} \text{ day}^{-1}$; Fig. 4a), as also during the spring of 2001 (early May 2001: 1.71×10^5 coccospheres $\text{m}^{-2} \text{ day}^{-1}$; late April 2001: 6.25×10^8 coccoliths $\text{m}^{-2} \text{ day}^{-1}$; Fig. 4a). Other major components were *U. sibogae* and *A. robusta* followed by *S. mediterranea*, *S. pulchra* and *C. leptoporus*, whereas *F. profunda* and *R. clavigera* also contributed to the coccolith flux (Fig. 4a, Supplementary Appendix 2). *F. profunda* coccolith flux had significantly high values in late March 2015 (maximum flux: 3.46×10^8 coccoliths $\text{m}^{-2} \text{ day}^{-1}$; Fig. 4a), while high fluxes of *U. sibogae* were documented during March to June (spring-early summer) with maxima occurring during late March 2015 (10.13×10^5 coccospheres $\text{m}^{-2} \text{ day}^{-1}$; 0.62×10^8 coccoliths $\text{m}^{-2} \text{ day}^{-1}$; Fig. 4a). Higher coccosphere fluxes of *Algirosphaera robusta* were present in early February 2001 (1.44×10^5 coccospheres $\text{m}^{-2} \text{ day}^{-1}$; Fig. 4a), followed by early April 2015 (0.55×10^5 coccospheres $\text{m}^{-2} \text{ day}^{-1}$; Fig. 4a); coccolith abundance of the species was practically negligible. Both large coccolith-bearing taxa *H. carteri* and *Pontosphaera* spp. contributed to the abundance with maximum fluxes of 0.23×10^5 coccospheres $\text{m}^{-2} \text{ day}^{-1}$, 0.04×10^8 coccoliths $\text{m}^{-2} \text{ day}^{-1}$ and 0.33×10^5 coccospheres $\text{m}^{-2} \text{ day}^{-1}$, 0.04×10^8 coccoliths $\text{m}^{-2} \text{ day}^{-1}$, respectively (Supplementary Appendix 2).

The input of *U. tenuis*, *D. tubifera*, *Scyphosphaera apsteinii* and *Gladiolithus flabelatus* was insignificant to the coccosphere and coccolith assemblages, as their abundance was <5% of coccosphere and <0.4% of coccolith fluxes (Fig. 4b), with total minor taxa coccolith flux (also including coccospheres converted to coccolith units) peaking in late March 2015 (6.63×10^8 coccoliths $\text{m}^{-2} \text{day}^{-1}$; Fig. 4b).

4.4. Ionian Sea

Total mass flux reached its highest values during May (late spring) of each annual cycle (peak in early May 2012; $756.72 \text{ mg m}^{-2} \text{day}^{-1}$, Fig. 2c), yet it was significantly lower throughout the rest of the year ($11\text{--}206 \text{ mg m}^{-2} \text{day}^{-1}$; Fig. 2c). The seasonal fluctuations were also tracked in total carbonate flux ($71 \text{ mg m}^{-2} \text{day}^{-1}$), total organic carbon ($15.21 \text{ mg m}^{-2} \text{day}^{-1}$) and total coccolithophore carbonate fluxes ($20.97 \text{ mg m}^{-2} \text{day}^{-1}$) with the maxima being recorded from February to May (late winter-early spring) of each year (Fig. 2c). Similarly, the lithogenic and PIC fluxes (up to 62% and 4.83% of the total mass flux) followed the same trend. The highest peak in lithogenic flux appeared in June 2015 ($127 \text{ mg m}^{-2} \text{day}^{-1}$; Fig. 2c), with a second one in February 2015 ($103 \text{ mg m}^{-2} \text{day}^{-1}$; Fig. 2c). PIC flux presented maximum values in February 2015 ($8.53 \text{ mg m}^{-2} \text{day}^{-1}$; Fig. 2d) followed by June 2015 ($5.91 \text{ mg m}^{-2} \text{day}^{-1}$; Fig. 2c).

Despite several sampling gaps, the total coccolithophore fluxes in the Ionian Sea displayed an overall seasonal pattern with higher values found mainly in late winter to spring (February-March) (Fig. 5a). The highest value during the period 2010–2012 occurred in late May 2012 (14.3×10^5 coccospheres $\text{m}^{-2} \text{day}^{-1}$; 1.53×10^8 coccoliths $\text{m}^{-2} \text{day}^{-1}$; Fig. 5a), followed by early May 2012 for coccospheres and early March 2012 for coccoliths (12.7×10^5 coccospheres $\text{m}^{-2} \text{day}^{-1}$; 1.34×10^8 coccoliths $\text{m}^{-2} \text{day}^{-1}$; Fig. 5a, Supplementary Appendix 2), while the minimum coccosphere flux values were recorded during late January 2011. For the interval 2014–2015, the total coccolithophore production was recorded from late January 2015 till early April 2015, with the highest total coccosphere flux peak occurring within late March 2015 and the coccolith flux maxima in late February 2015 (8.12×10^5 coccospheres $\text{m}^{-2} \text{day}^{-1}$; 1.27×10^8 coccoliths $\text{m}^{-2} \text{day}^{-1}$; Fig. 5a). The total coccosphere export flux was generally low from late October 2014 till early January 2015 (minimum values 0.35×10^5 coccospheres $\text{m}^{-2} \text{day}^{-1}$; 0.21×10^8 coccoliths $\text{m}^{-2} \text{day}^{-1}$; Fig. 5a).

Coccolithophore assemblage in the Ionian Sea was dominated by high abundances of *E. huxleyi*, ranging from 30–87% in coccosphere counting and 30–60% in coccoliths, with major coccosphere flux peak during late May 2012 (7.79×10^5 coccospheres $\text{m}^{-2} \text{day}^{-1}$; Fig. 5a) and coccolith flux maxima in early March of the same year (1.17×10^8 coccoliths $\text{m}^{-2} \text{day}^{-1}$; Fig. 5a). Similarly to the 2014–2015 coccolithophore export flux pattern, *E. huxleyi* major coccosphere (5.21×10^5 coccospheres $\text{m}^{-2} \text{day}^{-1}$) and coccolith (6.6×10^8 coccoliths $\text{m}^{-2} \text{day}^{-1}$) flux peaks occurred during late February-March 2015 (Fig. 5a). The taxa that also contributed to the total coccolithophore flux were *F. profunda* and *S.*

pulchra, accompanied by *U. sibogae*, *A. robusta*, *S. mediterranea* and *R. clavigera* (Supplementary Appendix 2). *Florisphaera profunda* displayed a peak during late April 2012 (0.55×10^8 coccoliths $\text{m}^{-2} \text{day}^{-1}$; Fig. 5a) and highest flux in early June 2015 (0.43×10^8 coccoliths $\text{m}^{-2} \text{day}^{-1}$; Fig. 5a). *Syracosphaera pulchra* maximum coccosphere flux was recorded in May 2012 (4.02×10^5 coccospheres $\text{m}^{-2} \text{day}^{-1}$; 0.03×10^8 coccoliths $\text{m}^{-2} \text{day}^{-1}$; Fig. 5a) with maximum coccolith flux values in late June 2015 (0.12×10^8 coccoliths $\text{m}^{-2} \text{day}^{-1}$; Fig. 5a) and a peak in late February 2015 (0.62×10^5 coccospheres $\text{m}^{-2} \text{day}^{-1}$; 0.10×10^8 coccoliths $\text{m}^{-2} \text{day}^{-1}$; Fig. 5a). The abundance of large coccolith-bearing species *H. carteri* and *Pontosphaera* spp. was 1.33×10^5 coccospheres $\text{m}^{-2} \text{day}^{-1}$, 0.03×10^8 coccoliths $\text{m}^{-2} \text{day}^{-1}$ and 0.03×10^5 coccospheres $\text{m}^{-2} \text{day}^{-1}$, 0.01×10^8 coccoliths $\text{m}^{-2} \text{day}^{-1}$, respectively (Supplementary Appendix 2). Other minor taxa (<1%) were *C. leptoporus*, *R. clavigera*, *U. tenuis* and *Calciosolenia* spp. Total minor taxa coccolith flux (also including coccospheres converted to coccolith units) exhibited highest peak during early May 2012 (0.47×10^8 coccoliths $\text{m}^{-2} \text{day}^{-1}$; Fig. 5b).

4.5. Black Sea

During the studied interval, total mass flux in the Black Sea exhibited seasonal fluctuations with highest value during late May 2008 ($348 \text{ mg m}^{-2} \text{day}^{-1}$; Fig. 2d) and early November 2007 ($182 \text{ mg m}^{-2} \text{day}^{-1}$; Fig. 2d). Total carbonate flux (max. late May 2008: $178.41 \text{ mg m}^{-2} \text{day}^{-1}$), total organic carbon flux (max. early November 2007: $42.38 \text{ mg m}^{-2} \text{day}^{-1}$) and total coccolithophore carbonate flux (max. early September 2008: $2 \text{ mg m}^{-2} \text{day}^{-1}$; calculation based only on total coccosphere countings converted to coccoliths), displayed an overall similar trend (Fig. 2d).

Total coccolithophore flux during late October 2007-early September 2008 at the Black Sea site was dominated by the species *E. huxleyi* (Supplementary Appendix 2). Due to extremely high *E. huxleyi* concentrations in the recovered samples (95–100%), coccosphere fluxes of this taxon have been calculated and then converted to coccoliths in order to be comparable with the coccolith results of the remaining investigated sites (max. late September 2008: 7.79×10^8 coccoliths $\text{m}^{-2} \text{day}^{-1}$; Fig. 6b). However, coccolith fluxes are considered to be underestimated, as they have been derived only from the counted coccospheres converted to coccoliths. The highest values were recorded during late November 2007 (320×10^5 coccospheres $\text{m}^{-2} \text{day}^{-1}$; Fig. 6a), followed by late September and late May 2008 (312×10^5 coccospheres $\text{m}^{-2} \text{day}^{-1}$ and 234×10^5 coccospheres $\text{m}^{-2} \text{day}^{-1}$ respectively; Fig. 6a, Supplementary Appendix 2). *Syracosphaera dilatata* was the single species apart from *E. huxleyi* recorded only in late June, with low both relative abundances (max 5.35%) and total cell densities (coccosphere flux max. 13×10^5 coccospheres $\text{m}^{-2} \text{day}^{-1}$; Fig. 6a).

5. Discussion

5.1. Eastern Mediterranean coccolithophore time series data: seasonal to interannual flux patterns

The investigated areas of the Eastern Mediterranean exhibit a seasonal surface productivity typical of subtropical-temperate zones (Malinverno et al., 2009). Coccolithophore production and coccolithophore carbonate flux displayed maxima within late winter-early summer (February-June), corresponding to increased Chl-a and the highest values of total mass and carbonate fluxes (Fig. 2, Supplementary Fig. 1). This period is characterised by precipitation peaks associated with the external input of nutrients through riverine runoff or precipitation-mediated atmospheric sources that support elevated coccolithophore productivity (Malinverno et al., 2009). Chl-a concentrations have been shown before to be positively correlated with coccolithophore fluxes (e.g. Broerse et al., 2000a), however this is not always the case (e.g. Ziveri et al., 2000). Except coccolithophores, Chl-a peaks can be related to the production of diatoms, pico-phytoplankton and naked nannoplankton (Boldrin et al., 2002; Malinverno et al., 2014; Socal et al., 1999). In contrast, the positive shifts in PIC flux imply enhanced contribution from pelagic calcifying organisms (i.e., coccolithophores; Westbroek et al., 1993; Holligan et al., 2010; Rembauville et al., 2016) to the carbonate export, clearly supporting a late winter-spring coccolithophore productivity pattern in the Aegean and Ionian Seas (Fig. 2)

A comparative description of inter-annual coccolithophore export in the North Aegean, Ionian and Cretan Seas reveals an increasing coccolithophore flux pattern within at least two annual cycles in every site (North Aegean: 2011 and 2015; Ionian: 2011–2012 and 2015; Cretan Sea: 2001 and 2015; Figs. 7a-c). Highest values occurred during 2015, including an outstanding peak documented in late winter-early spring 2015 (February-March) in the North Aegean site. The amplified coccolithophore productivity during February-March 2015 is verified by the high PIC flux and the increased Chl-a concentrations according to the satellite data (Fig. 2a). Karatsolis et al. (2016) have also observed an analogous pattern in the water column coccolithophore assemblages during March 2014, discussing a positive correlation of the total coccolithophore flux increment with enhanced nutrients exports associated to the nutrient-rich surface BSW layer.

In the oligotrophic Ionian Sea, the coccolithophore productivity pattern was consistent with the rest of the sites. The recorded maxima in coccolithophore fluxes were comparable between the studied years (2010–2012 and 2014–2015), with major peaks observed in late winter-spring convective mixing period (Figs. 5a, 7c), in accordance with previous reports on the patterns of marine productivity and PIC fluxes in the area (D’Ortenzio and Ribera d’Alcala, 2009; Patara et al., 2009; Stavrakakis et al., 2013; Malinverno et al., 2014). Gogou et al. (2016) linked the isolated productivity peak of June-July (2012), to the impact of particularly strong cold and dry northerly winter winds that triggered intense

convection mixing causing the observed increased biogenic fluxes in the following summer months (Fig. 5).

Overall, lithogenic fluxes were positively correlated with coccolith export fluxes; hence, their increased contribution to the total mass flux (reaching 70% and 62%, in the N. Aegean and Ionian Seas respectively) cannot be attributed to resuspension, as both North Aegean and Ionian mooring depths were much shallower than the sea bed (see Table 1). Apparently, the increased precipitation in the North Aegean during winter has triggered increased river runoffs in the area, which have drastically affected the lithogenic flux and the contemporaneous increase in coccolithophore productivity through the concomitant increase in nutrient inputs (Skampa et al., 2019). In contrast, the Ionian Sea is characterised by the absence of important riverine inputs; thus, aeolian transport is probably the prevailing process transferring lithogenic material in the marine environment (Stavrakakis et al., 2013). The occurrence of diatom species, typical from the dry lake beds of North Africa, in Ionian sediment traps, demonstrate the importance of atmospheric inputs of (bio)lithogenic material, implying a common sedimentation mechanism related to the packaging of particles in faecal pellets from suspension feeders or the ballasting role of Saharan dust (Stavrakakis et al., 2013; Malinverno et al., 2014).

The observed seasonality pattern of the total coccolith flux in the Cretan Sea, suggested an increased productivity season during spring months (March-May, Stavrakakis et al., 2000; Triantaphyllou et al., 2004; present study). The late March 2015 extreme peak in coccolith flux demonstrated in the present study (Fig. 6b), represents a general feature of the area (see also South Cretan Margin; Malinverno et al., 2009; Karageorgis et al., 2018) and is clearly documented in high PIC flux and the Chl-a satellite dataset (Fig. 2b; Supplementary Fig. 1). The sediment trap of the Cretan Sea presented subordinate lithogenic flux, reaching up to 55% of the total mass flux; with the major source of the lithogenic particles to be associated with the atmospheric deposition (Theodosi et al., 2019). Yet, as the Cretan Sea mooring was much closer to the seafloor (see Table 1), we cannot exclude that a part of the coccolith flux might represent resuspended material. In order to avoid imprints of coccolith resuspension, countings of coccolith fluxes during 2001–2002 have been performed at the shallower trap (500 m depth; Triantaphyllou et al., 2004); samples from the shallower trap were not available during the 2015 sampling interval and coccolith fluxes were estimated at 100 m above the bottom. Still, the coccolith flux displayed the exact same pattern as the coccosphere fluxes (Fig. 4), depicting the surface productivity (Malinverno et al., 2009) and therefore minimizing any assumption concerning lateral transport impacts.

Black Sea coccolithophore flux did not track the same seasonal productivity pattern with the Eastern Mediterranean sites, as the highest values were recorded during both the fall (November 2007, September 2008) and spring period (May 2007) at the end of the Chl-a increase (Fig. 2; Supplementary Fig. 1), with a Chl-a maximum associated with the preceding diatom bloom

(Bouloubassi et al., 2010). None of the investigated Aegean and Ionian sites could be compared to the prominently high Black Sea fluxes in late November 2007, which even reached 320×10^5 coccospheres $\text{m}^{-2} \text{day}^{-1}$ (Fig. 6a) and at least 7.79×10^8 coccoliths $\text{m}^{-2} \text{day}^{-1}$ (Fig. 6b, coccolith flux derived only from the counted coccospheres converted to coccoliths). Apparently, this is in accordance with the highly productive and nutrient-enriched Black Sea waters (e.g., Bouloubassi et al., 2010) and the excessive precipitation levels that enhance the riverine nutrient input especially during fall and spring (Siokou-Frangou et al., 2009; present study, Supplementary Fig. 1).

5.2. Coccolithophore assemblage composition

(1) *Emiliania huxleyi*

The total coccolithophore flux pattern in the Aegean and Ionian Seas presented increased values during late winter-early summer (February-June), mostly reflecting the seasonal peak of *E. huxleyi* (Figs. 7a-c; highest average coccolith abundance ~70% recorded in the North Aegean Sea), in agreement with previous sediment trap studies in the area (Triantaphyllou et al., 2004; Malinverno et al., 2009, 2011). The *E. huxleyi* is a taxon that can thrive well under a wide range of temperatures and salinities, being most abundant in the surface layers but it is also found in relative deeper layers of the photic zone (Okada and McIntyre, 1979; Bukry, 1974; Roth and Colbourn, 1982; Okada and Wells, 1997). In subtropical-temperate areas like the Eastern Mediterranean the nutrient increase during winter mixing causes spring bloom conditions with high coccolithophore fluxes, dominated by *E. huxleyi* (Broerse et al., 2000b, c; Malinverno et al., 2009). Indeed, the presence of *E. huxleyi* has been documented in the Aegean Sea water column during the late winter-early spring period associated with the increased river runoff and winter overturning of the water column (Triantaphyllou et al., 2002, 2004, 2014; Dimiza et al., 2008, 2015; Skampa et al., 2019), following the fertilization of the photic zone mostly with macronutrients during SST minima (Souvermezoglou et al., 2014; Lagaria et al., 2017). Although riverine inputs are negligible in the Cretan Sea, the high N/P ratio (Tselepides et al., 2000), resulting in an increase of phosphorus limitation, may have enhanced the dominance of *E. huxleyi* (up to 60%) in the coccolithophore assemblages (Figs. 4a, 7b), as this taxon is known to flourish under favourable conditions with low phosphate and high nitrate concentrations (Tyrell and Taylor, 1995; Riegman et al., 1998). The prevalence of *E. huxleyi* is also prominent in the Ionian Sea sediment trap (average coccolith abundance slightly higher than 45%; Fig. 7c) but with much lower fluxes when compared to the other sites (Figs. 3–5); the higher values occurred during spring (March-May), showing an inverse pattern to the species productivity to the SST (15.4–17.9°C; Supplementary Fig. 1).

Emiliania huxleyi practically comprised the monospecific coccolithophore assemblage (~100% relative abundance) of the Black Sea sediment trap leading to extremely high coccosphere fluxes in

November 2007, associated with enhanced riverine nutrient inputs during the precipitation maximum (Fig. 6, Supplementary Fig. 1).

(2) *Florisphaera profunda*

Florisphaera profunda is restricted to the light-limited, lower euphotic zone of the tropical and subtropical environments (Okada and Honjo, 1973; Winter et al., 1994; Sprengel et al., 2000; Kinkel et al., 2000). This species has proven to be a reliable proxy to locate the nutricline-thermocline as well as for paleoproductivity, indicating the Deep Chlorophyll Maximum (Molfinio and McIntyre, 1990; Sprengel et al., 2000; Malinverno et al., 2014). Its high abundance strongly suggests the presence of water column stratification (Molfinio and McIntyre, 1990; Colmenero-Hidalgo et al., 2004; Triantaphyllou et al., 2004, 2009; Dimiza et al., 2015). In the North Aegean time-series, *F. profunda* presented a seasonal pattern with higher fluxes during the summer months (June-August). A second peak occurred within late winter-early spring (February-March), associated with the increased precipitation and consequent riverine inputs (Supplementary Fig. 1), leading to an enhancement of the water column stratification (Triantaphyllou, 2014). *Florisphaera profunda* coccolith flux in the Cretan Sea was in correspondence with the total coccolith flux (Fig. 7b), displaying prominently higher values within 2015 in comparison to the 2001 data set, with major peak during early March. The simultaneous high abundance of this deep-water species along with *E. huxleyi* suggests high coccolithophore production throughout the water column (Triantaphyllou et al., 2004). High values of *F. profunda* were recorded during late spring-early summer (April-June) in the Ionian Sea, implying the presence of stratified deep-water layers (e.g., Ziveri et al., 2000b; Triantaphyllou et al., 2004; Malinverno et al., 2014).

(3) *Syracosphaera* spp.

Syracosphaera pulchra seems to have an oligotrophic-mesotrophic distribution (Ziveri et al. 2000a, b; Triantaphyllou et al., 2004; Crudeli et al., 2006) and indicates warmer surface waters and low salinities (Flores et al., 1999; Colmenero-Hidalgo et al., 2004; Dimiza et al., 2008, 2015; Karatsolis et al., 2016). The ecological affinities of this taxon are consistent with the seasonally controlled fluctuations in our sediment trap records, where *S. pulchra* exhibited flux peaks associated with increasing SSTs (Supplementary Fig. 1). Particularly for the North Aegean an additional *S. pulchra* increment in late fall 2014 fits nicely with precipitation maxima, in agreement with Malinverno et al. (2009, 2014), who indicated that *S. pulchra* corresponds to the interval of maximum rainfall.

Syracosphaera dilatata in the Black Sea, even though extremely low in abundances, was similarly related to the increased SSTs (May-September 2008).

Coccolith flux of *Syracosphaera mediterranea* reached its higher values during February-March in the Aegean and Ionian Seas, mostly following the concurrent increased total coccolithophore flux in

the high productivity season (Figs. 3–5). Whenever found with *R. clavigera* (e.g., Cretan Sea; Fig. 4a) it might document a well-developed surface community (Malinverno et al., 2009).

(4) *Algirosphaera robusta*

Algirosphaera robusta inhabits the deep photic zone of tropical to intermediate environments (e.g., Okada and Honjo, 1973; Okada and McIntyre, 1979; Knappertsbusch, 1993). This species is also associated with a limited increase in the concentration of nutrients (Broerse et al., 2000c) and is considered as a deep dweller, even if it is occasionally present in surface waters (e.g., Dimiza et al., 2008). *Algirosphaera robusta* higher fluxes in the North Aegean time series were associated with the lower SST interval (February to early April 2015; Fig. 7a, Supplementary Fig. 1) in accordance with the species preference in the North Aegean lower photic zone during low SSTs (Dimiza et al., 2015). In the Cretan and Ionian Seas, it thrived during different intervals through the whole year 2001, with the major peak in late February, in agreement to Malinverno et al. (2009). It seems that this is an overall feature for the Eastern Mediterranean region; the significant peak of *A. robusta* takes place during winter (December-February), when the surface mixed layer is deeper and nutrients are likely more easily diffused to the lower photic zone from deeper water layers, below the nutricline (~150 m; Souvermezoglou and Krasakopoulou, 2002).

(5) *Umbilicosphaera sibogae*:

Umbilicosphaera sibogae is a proxy of saline, warm and oligotrophic waters (Wells and Okada, 1997; Flores et al., 1999; Andrleit & Rogalla, 2002; Baumann et al., 2016). In the North Aegean Sea, this taxon is found to follow the SST increase (Fig. 3c, Supplementary Fig. 1). In accordance with Malinverno et al. (2009), *U. sibogae* exhibited an increase during the interval of high total coccolith flux (March 2015) in the Cretan Sea, responding positively to the SST increment and the nutrient availability resulting from the seasonal water column mixing. *Umbilicosphaera sibogae* preference to warm waters is more prominent in the Ionian time series with maxima during summer (Figs. 5a, 7c).

5.3. Factors controlling the coccolithophore flux patterns in the Aegean and Ionian Seas

Seasonal shifts in the oceanographic parameters and biogenic fluxes (Fig. 2, Supplementary Fig. 1) can alter the composition of coccolithophore assemblages, as tracked by coccolith export production, with consequent impacts on the carbonate system (Ziveri et al., 2007). The North Aegean Sea presented the highest values in biogenic fluxes and total coccolithophore CaCO_3 flux among all sites, while the peak in total carbonate flux featured the Cretan Sea time-series during late March 2015 is well correlated with the simultaneous coccolithophore carbonate flux increment (Fig. 2). Interestingly, the Black Sea presented the lowest total coccolithophore CaCO_3 flux among the investigated areas despite the extremely high *E. huxleyi* flux values (Figs. 2a–d). Apparently this is linked not only to the

underestimated coccolith fluxes but mostly to the species with much lower coccolith mass, in comparison to taxa bearing larger coccoliths (e.g., *Pontosphaera* spp., *S. apsteinii*, *H. carteri*), which contribute to carbonate export in the Eastern Mediterranean sites (Fig. 8). Hence, the carbonate mass percentage of robust coccolith taxa such as *S. apsteinii* (up to: 10% in North Aegean, 17% in Cretan Sea, 8% in Ionian), *Pontosphaera* spp. (up to: 45% in North Aegean, 39% in Cretan Sea, 65% in Ionian) and *H. carteri* (up to: 20% in North Aegean, 30% in Cretan Sea, 42% in Ionian) must have influenced the increased total coccolithophore carbonate flux (Figs. 8a–c), despite their low contribution in the coccolithophore assemblage. In contrast, even though *E. huxleyi* was dominating in the coccolith fluxes, its small mass resulted to the low carbonate contribution of the species especially in the Cretan and Ionian sites (Figs. 8a–c).

When comparing all three Aegean and Ionian sites during a single annual cycle (2015), it is evident that North Aegean total coccolith flux was not only considerably higher than those recorded in the Ionian and Cretan Seas but also displayed a substantial difference between the cold (November–April) and the warm (May–October) season (Fig. 9). This difference is related to the spreading of colder and less saline nutrient-enriched BSW inputs (Zervakis et al., 2000) and land-derived organic matter due to riverine discharges (Poulos et al., 1997; Roussakis et al., 2004), which enhance the coccolithophore productivity of the upper water column (e.g., Dimiza et al., 2015; Karatsolis et al., 2016; Skampa et al., 2019). In the Cretan Sea, the maxima in coccolithophore productivity observed in early spring (Fig. 9) are likely to be associated with the fertilization in the upper photic zone due to the intrusion of the Transitional Mediterranean Water (TMW), coming from the mid-depths of the Eastern Mediterranean through the eastern and western Cretan Arc Straits (Lykousis et al., 2002; Triantaphyllou et al., 2004). Although the Ionian Sea time-series displayed a similar seasonal pattern with the export flux maxima occurring during late winter–early summer (February–March and May–June) in agreement with the convective mixing period (D’Ortenzio and Ribera d’Alcala, 2009; Stavrakakis et al., 2013), seasonality proved to have minimum impact on the coccolith fluxes between the cold (November–April) and the warm (May–October) period (Fig. 9), in a continually oligotrophic setting (e.g., Souvermezoglou et al. 1999).

Evidently, the export fluxes in the studied NE–SW mooring transect are strongly dependent on the nutrient influx, the vertical mixing and/or the influence of episodic dust input events. The latter affect mostly the Ionian and Cretan Seas, contributing to new production (Herut et al., 2005; Krom et al., 2004; Schulz et al., 2012), even though their role in effectively fertilizing the surface waters of the Eastern Mediterranean has been under discussion (Herut et al., 1999; Krom et al., 2005). In general, the Eastern Mediterranean Sea receives massive airborne plumes of desert dust from the Sahara during the whole year (Bergametti et al., 1989; Moulin et al., 1997) that form a pathway for nutrient inputs in the nutrient-depleted upper water column (Rutten et al., 2000; Kouvarakis et al., 2001; Markaki et al., 2003; Tsagaraki et al., 2017) and enhance coccolithophore productivity (Ziveri et al.,

2000b; Triantaphyllou et al., 2004; present study). However, as precipitation maxima occur during the late winter-spring period (February-May), it is evident that most of the annual dust input in Ionian and Cretan Seas occurs as wet dust deposition (65-80%, Molinaroli et al., 1993; partially documented in the present study by the increased lithogenic fluxes, Figs. 2b-c). Natural plankton communities form abundant and fast-sinking aggregates when exposed to Saharan dust deposition that triggers an increase in the coccolith sinking rate and maximum coccolithophore export fluxes (Guerreiro et al., 2017; Van der Jagt et al., 2018). Thus, the rapid vertical mass transfer recorded during spring in the Cretan Sea can be attributed to the formation of big aggregates with atmospheric dust particles (Theodosi et al., 2019).

6. Conclusions

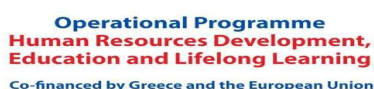
The current study provides important insight into the spatio-temporal variability and environmental control of coccolithophore export fluxes in the North Aegean Sea (Athos Basin), the Cretan Sea (South Aegean) and the Ionian Sea (Nestor site), while these fluxes are further compared to the corresponding ones occurring in the southwestern Black Sea. The main findings of this study may be summarized as follows:

- All analysed sediment trap data in the Aegean and Ionian Seas, are characterised by seasonally-controlled coccolithophore fluxes with maxima recorded within late winter-early summer during the mixing phase of the water column, with PIC maxima strongly supporting enhanced productivity. *Emiliania huxleyi* is the dominant species in all investigated sites, prominently affecting the coccolithophore export fluxes. Other taxa, such as *F. profunda*, *S. pulchra*, *A. robusta* and *U. sibogae* contribute to the assemblage composition but with much lower relative abundances.
- Coccolithophore fluxes demonstrate an increasing trend within the last 15 years. The North Aegean Sea exhibits considerably higher total coccolith flux with respect to the rest of the study areas, due to the prominent seasonal peak of *E. huxleyi* (February-March). The Cretan (March-May) and Ionian Seas (February-March and May-June) displayed a slightly delayed peak. In contrast to the Mediterranean settings, the Black Sea sediment trap time-series data indicate monospecific, i.e., *E. huxleyi*, extreme fluxes with maxima rising during late summer-fall. Eastern Mediterranean coccolithophore carbonate fluxes follow the total mass flux pattern, while the Black Sea coccolithophore carbonate flux is the lowest one, mostly associated with the low mass contribution of *E. huxleyi* coccoliths.
- The export fluxes in the studied mooring transect reveal a decreasing pattern towards the southeastern Ionian Sea, being strongly dependent on the vertical water column mixing occurring in the North Aegean Sea during winter and/or the influence of episodic dust input

events in the Ionian and Cretan Seas. In the latter areas, Saharan dust might contribute to higher coccolithophore productivity and/or the formation of fast-sinking aggregates during March-May, when maximum coccolithophore export fluxes appear.

Acknowledgements

The funding for the fulfilment of this study was provided by: the Greek National Project KRIPIS (Integrated Observatories in the Greek Seas - IO, HCMR-MIS 451724; NSRF); the European Research Project MedEcos (EraNet/MarinERA, EU/FP6); the KM3NET/FP6-DG Environment; the PERSEUS FP7 EU Project; the SESAME FP6 EU Project; the IKYDA program of DAAD (project no 57260124 AegeanCocco). We acknowledge support of this work by the project “PANhellenic infrastructure for Atmospheric Composition and climatE change” (MIS 5021516) which is implemented under the Action “Reinforcement of the Research and Innovation Infrastructure”, funded by the Operational Programme “Competitiveness, Entrepreneurship and Innovation” (NSRF 2014–2020) and co-financed by Greece and the European Union (European Regional Development Fund). The constructive criticism and comments of the two anonymous reviewers concerning the improvement of the current manuscript are appreciated. English language has been corrected by Dr. Alexander Robinson, Complutense University of Madrid. The first author E. Skampa has been granted with a scholarship from the State Scholarships Foundation. This research is co-financed by Greece and the European Union (European Social Fund- ESF) through the Operational Programme «Human Resources Development, Education and Lifelong Learning» in the context of the project “Strengthening Human Resources Research Potential via Doctorate Research” (MIS-5000432), implemented by the State Scholarships Foundation (IKY)



References

- Acker, J. G., Leptoukh, G., 2007. Online Analysis Enhances Use of NASA Earth Science Data”. Eos, Trans. AGU 88, 14–17.
- Andruleit, H., Rogalla, U. 2002. Coccolithophores in surface sediments of the Arabian Sea in relation to environmental gradients in surface waters. Marine Geology 186, 505–526.
- Baumann, K.-H., 2004. Importance of size measurements for coccolith carbonate flux estimates. Micropaleontology 50, 35–43.

- Baumann, K.-H., Andruleit, H., Bockel, B., Geisen, M., and Kinkel, H., 2005. The significance of extant coccolithophores as indicators of ocean water masses, surface water temperature, and paleoproductivity: a review. *Paläontologische Zeitschrift* 79, 93–112.
- Baumann, K.-H., Andruleit, H.A., Samtleben, C., 2000. Coccolithophores in the Nordic Seas: comparison of living communities with surface sediment assemblages. *Deep-Sea Research Part II* 47, 1743–1772.
- Baumann, K.-H., Saavedra-Pellitero, M., Böckel, B., Ott, C., 2016. Morphometry, biogeography and ecology of *Calcidiscus* and *Umbilicosphaera* in the South Atlantic. *Revue de Micropaléontologie* 59 (3), 239–251.
- Bairbakhish, A.N., Bollmann, J., Sprengel, C., Thierstein, H.R., 1999. Disintegration of aggregates and coccospheres in sediment trap samples. *Marine Micropaleontology* 37, 219–640 223.
- Bergametti, G., Dutot, A.-L., Buat-Ménard, P., Losno, R., Remoudaki, E., 1989. Seasonal variability of the elemental composition of atmospheric aerosol particles over the northwestern Mediterranean, *Tellus B: Chemical and Physical Meteorology* 41, 3, 353–361, DOI: 10.3402/tellusb.v41i3.15092
- Boeckel, B., Baumann, K.-H., 2008. Vertical and lateral variations in coccolithophore community structure across the subtropical frontal zone in the South Atlantic Ocean. *Marine Micropaleontology* 67, 255–273.
- Boldrin, A., Miserocchi, S., Rabitti, S., Turchetto, M. M., Balboni, V., Socal, G. 2002. Particulate matter in the southern Adriatic and Ionian Sea: characterisation and downward fluxes, *Journal of Marine Systems* 33–34, 389–410.
- Bouloubassi, I., Gogou, A., Plakidi, E., Lorre, A., Kambouri, S., Stavrakaki, I., Stavrakakis, S., 2010. Biomarkers as tracers of organic carbon fluxes in the SW Black Sea: a 1yr sediment trap experiment (SESAME project). *Rapp. Comm. Int. Mer. Médit.* 39, 224.
- Broerse, A.T.C., 2000c. Coccolithophore export production in selected ocean environments: seasonality, biogeography, carbonate production. Amsterdam: VU, 2000. 185 p.
- Broerse, A.T.C., Brummer, G.-J.A., Brummer, Van Hinte, J.E., 2000b. Coccolithophore export production in response to monsoonal upwelling off Somalia (northwestern Indian Ocean). *Deep-Sea Research Part II* 47, 2179–2205.
- Broerse, A.T.C., Ziver, P., Van Hinte, J.E., Honjo, S., 2000a. Coccolithophore export production, species composition, and coccolith- CaCO_3 fluxes in the NE Atlantic (34°N 21°W and 48°N 21°W). *Deep-Sea Research Part II* 47, 1877–1905.
- Bukry D., 1974. Coccoliths as paleosalinity indicators-evidence from Black Sea. *American Association of Petroleum Geologist. Memoir* 20, 353–633.

- 758 Cachão, M., Moita, T., 2000. *Coccolithus pelagicus*, a productivity proxy related to moderate fronts
759 off Western Iberia. *Marine Micropaleontology* 39 (1/4), 131–155.
- 760 Casotti, R., Landolfi, A., Brunet, C., D’Ortenzio, F., Mangoni, O., Ribera d’Alcala, M., and Denis,
761 M., 2003. Composition and dynamics of the phytoplankton of the Ionian Sea (eastern Mediterranean),
762 *Journal of Geophysical Research* 108, 8116, doi:10.1029/2002JC001541.
- 763 Cokacar, T., Oguz, T., Kubilay, N., 2004. Satellite-detected early summer coccolithophore blooms
764 and their interannual variability in the Black Sea. *Deep-Sea Research Part I* 51, 1017–1031.
- 765 Colmenero-Hidalgo, E., Flores, J.-A., Sierro, F.J., Bárcena, M.Á., Löwemark, L., Schönfeld, J.,
766 Grimalt, J.O., 2004. Ocean surface water response to short-term climate changes revealed by
767 coccolithophores from the Gulf of Cadiz (NE Atlantic) and Alboran Sea (W Mediterranean).
768 *Palaeogeography, Palaeoclimatology, Palaeoecology* 205, 317–336.
- 769 Crombet, Y., Leblanc, K., Qu’éguiner, B., Moutin, T., Rimmelin, P., Ras, J., Claustre, H., Leblond,
770 N., Oriol, L., and Pujo-Pay, M., 2011. Deep silicon maxima in the stratified oligotrophic
771 Mediterranean Sea. *Biogeosciences* 8, 459–475, doi:10.5194/bg-8-459-2011.
- 772 Crudeli, D., Young, J.R., Erba, E., Geisen, M., Ziveri, P., de Lange, G.J., Slomp, C.P., 2006. Fossil
773 record of holococcoliths and selected hetero-holococcolith associations from the Mediterranean
774 (Holocene–late Pleistocene): Evaluation of carbonate diagenesis and palaeoecological–
775 palaeocenographic implications. *Palaeogeography, Palaeoclimatology, Palaeoecology* 237, 191– 224.
- 776 D’Ortenzio, F., Ribera d’Alcalà, M., 2009. On the trophic regimes of the Mediterranean Sea: a satellite
777 analysis. *Biogeosciences* 6, 139–148.
- 778 Danovaro, R., Carugati, L., Boldrin, A., Calafat, A., Canals, M., Fabres, J., Finlay, K., Heussner, S.,
779 Miserocchi, S., Sanchez-Vidal, A., 2017. Deep-water zooplankton in the Mediterranean Sea: Results
780 from a continuous, synchronous sampling over different regions using sediment traps. *Deep-Sea*
781 *Research Part I* 126, 103–114.
- 782 Dimiza M., Triantaphyllou, M.V., Dermitzakis, M.D., 2008. Seasonality and ecology of living
783 coccolithophores in E. Mediterranean coastal environments (Andros Island, Middle Aegean Sea).
784 *Micropaleontology* 54, 159–175
- 785 Dimiza M., Triantaphyllou, M.V., Malinverno E., Psarra S., Karatsolis BT., Mara P., Lagaria A.,
786 Gogou A., 2015. The composition and distribution of living coccolithophores in the Aegean Sea (NE
787 Mediterranean). *Micropaleontology* 61, 521–540.
- 788 Fischer, G., Karakas, G., 2009. Sinking rates of particles in biogenic silica- and carbonate dominated
789 production systems of the Atlantic Ocean: implications for the organic carbon fluxes to the deep
790 ocean. *Biogeosciences* 6, 85–102.

- 791 Flores, J.A., Gersonde, E., Sierro, F.J., 1999. Pleistocene fluctuations in the Aguhlias Current
792 Retroflection based on the calcareous plankton record. *Marine Micropalaeontology* 37, 1–22.
- 793 Forbes, J.R., Macdonald, R.W., Carmack, E.C., Iseki, K., O'Brien, M.C., 1992. Zooplankton
794 retained in sequential sediment traps along the Beaufort Sea shelf break during winter. *Canadian*
795 *Journal of Fisheries and Aquatic Sciences* 49, 663–667.
- 796 Georgopoulos, D., Chronis, G., Zervakis, V., Lykousis, V., Poulos, S., Iona, A., 2000. Hydrology and
797 circulation in the Southern Cretan Sea during the CINCS experiment (May 1994–September 1995).
798 *Progress in Oceanography* 46, 85–112.
- 799 Georgopoulos, D., Theocharis, A., Zodiatis, G., 1989. Intermediate water formation in the Cretan Sea
800 (South Aegean Sea). *Oceanologica Acta* 12, 353–359.
- 801 Gislason, A., Asithorsson, O.S., 1992. Zooplankton collected by sediment trap moored in deep water
802 south of Iceland. *Sarsia* 77, 219–224.
- 803 Gogou, A., Stavrakakis, S., Triantaphyllou, M., Paraskos, F., Parinos, C., Dimiza, M., Kambouri, G.,
804 Lykousis, V., 2016. Seasonal and interannual variability of sinking particulate matter in the deep
805 Ionian Sea: ecological and biogeochemical perspectives. *Rapp. Comm. int. Mer Médit.*, 41.
- 806 Guerreiro, C.V., Baumann, K.-H., Brummer, G.-J., A., Fisher, G., Korte, L.F., Merkel, U., Sá, C., de
807 Stigter, H., Stuut, J.-B.W., 2017. Coccolithophore fluxes in the open tropical North Atlantic: influence
808 of thermocline depth, Amazon water, and Saharan dust. *Biogeosciences* 14, 4577–4599.
- 809 Hay, B.J., Honjo, S., Kempe, S., Ittekkot, V.A., Degens, E.T., Konuk, T., Izdar, E., 1990. Interannual
810 variability in particle flux in the southwestern Black Sea. *Deep Sea Research Part I* 37, 911–928.
- 811 Herut, B., Krom, M.D., Pan, G., Mortimer, R., 1999. Atmospheric input of nitrogen and phosphorous
812 to the Southeast Mediterranean: sources, fluxes, and possible impact. *Limnology and Oceanography*
813 44 (7), 1683–1692.
- 814 Herut, B., Zohari, T., Krom, M.D., Fauzi, R., Mantoura, C., Pitta, P., Psarra, S., Rassoulzadegan, F.,
815 Tanaka, T., Thingstad, T.F., 2005. Response of East Mediterranean surface water to Saharan dust:
816 On-board microcosm experiment and field observations. *Deep-Sea Research Part II* 52, 3024–3040.
- 817 Holligan, P.M., Charalampopoulou, A., Hutson, R., 2010. Seasonal distributions of the
818 coccolithophore, *Emiliania huxleyi*, and of particulate inorganic carbon in surface waters of the Scotia
819 Sea. *Journal of Marine Systems* 82, 195–205.
- 820 Honjo, S., 1976. Coccoliths: production, transportation and sedimentation. *Marine Micropaleontology*
821 1, 65–79.
- 822 Humborg, C., Ittekkot, V., Cociasu, A., Bodungen, B.V., 1997. Effect of Danube River dam on Black
823 Sea biogeochemistry and ecosystem structure. *Nature* 386, 385–388.

- 824 Ignatiades, L. 2005: Scaling the trophic status of the Aegean Sea, eastern Mediterranean, *Journal of*
825 *Sea Research* 54 (1), 51–57.
- 826 Ignatiades, L., Gotsis-Skretas, O., Pagou, K., Krasakopoulou, E., 2009. Diversification of
827 phytoplankton community structure and related parameters along a large-scale longitudinal east–west
828 transect of the Mediterranean Sea. *Journal of Plankton Research* 31, 411–428.
- 829 Ignatiades, L., Psarra, S., Zervakis, V., Pagou, K., Souvermezoglou, E., Assimakopoulou, G., Gotsis-
830 Skretas, O., 2002. Phytoplankton size-based dynamics in the Aegean Sea (Eastern Mediterranean).
831 *Journal of Marine Systems* 36, 11–28.
- 832 Karageorgis, A. P., Georgopoulos, D., Kanellopoulos, T. D., Mikkelsen, O. A., Pagou, K.,
833 Kontoyiannis, H., Pavlidou, A., Anagnostou, C., 2012. Spatial and seasonal variability of particulate
834 matter optical and size properties in the Eastern Mediterranean Sea. *Journal of Marine Systems* 105–
835 108, 123–134.
- 836 Karageorgis, A.P., Kontoyiannis, H., Stavrakakis, S., Krasakopoulou, E., Gogou, A., Papadopoulos,
837 A., Kanellopoulos, Th.D., Rousakis, G., Malinverno, E., Triantaphyllou, M.V., Lykousis, V., 2018.
838 Particle dynamics and fluxes in canyons and open slopes of the southern Cretan margin (Eastern
839 Mediterranean). *Progress in Oceanography* 169, 33–47.
- 840 Karatsolis B.-Th., Triantaphyllou M.V., Dimiza M. D., Malinverno E., Lagaria A., Mara P.,
841 Archontikis O., Psarra S., 2016. Coccolithophore assemblage response to Black Sea Water inflow into
842 the North Aegean Sea (NE Mediterranean). *Continental Shelf Research* 149, 138–150.
- 843 Kleijne, A., 1991. Holococcolithophorids from the Indian Ocean, Red Sea, Mediterranean Sea and
844 North Atlantic Ocean. *Marine Micropaleontology* 17, 1–76.
- 845 Knappertsbusch, M., 1993. Geographic distribution of living and Holocene coccolithophores in the
846 Mediterranean Sea. *Marine Micropaleontology* 21, 219–247.
- 847 Koebrich, M.I., Baumann, K.-H., Fischer, G., 2016. Seasonal and inter-annual dynamics of
848 coccolithophore fluxes from the upwelling region off Cape Blanc, NW Africa. *Journal of*
849 *Micropalaeontology* 35, 103–116.
- 850 Korotaev, G., Oguz, T., Nikiforov, A., Koblinsky, C., 2003. Seasonal, interannual, and mesoscale
851 variability of the Black Sea upper layer circulation derived from altimeter data. *Journal of*
852 *Geophysical Research: Oceans* 108 (C4), 3122
- 853 Kouvarakis, G., Mihalopoulos, N., Tselepides, T., Stavrakakis, S., 2001. On the importance of
854 atmospheric inputs of inorganic nitrogen species on the productivity of the eastern Mediterranean Sea.
855 *Global Biogeochemical Cycles* 15, 805–818.

- 856 Krom, M., Herut, B., and Mantoura, R.F.C., 2004. Nutrient budget for the Eastern Mediterranean:
857 Implications for phosphorus limitation. *Limnology and Oceanography* 49, 1582–1592.
- 858 Krom, M.D., Thingstad, T.F., Brenner, S., Carbo, P., Drakopoulos, P., Fileman, T.W., G.A.F., Groom,
859 S., Herut, B., Kitidis, V., Kress, N., Law, C.S., Liddicoat, M.I., Mantoura, R.F.C., Pasternal, A., Pitta,
860 P., Polychronaki, T., Psarra, S., Rassoulzadegan, F., Skjodal, E.F., Spyres, G., Tanaka, T., Tselepidis,
861 A., Wassman, P., Wexels Riser, C., Woodward, E.M.S., Zodiatis, G., Zohary, T., 2005. Summary and
862 overview of the CYCLOPS P addition Lagrangian experiment in the eastern Mediterranean. *Deep-Sea*
863 *Research Part II* 52, 3090–3108.
- 864 Lagaria, A., Mandalakis, M., Mara, P., Frangoulis, C., Karatsolis, B.-T., Pitta, P., Triantaphyllou, M.,
865 Tsiola, A., Psarra, S., 2017. Phytoplankton variability and community structure in relation to
866 hydrographic features in the NE Aegean frontal area (NE Mediterranean Sea). *Continental Shelf*
867 *Research* 149, 124–137.
- 868 Lagaria, A., Psarra, S., Gogou, A., Tuğrul, S., Christaki, U., 2013. Particulate and dissolved primary
869 production along a pronounced hydrographic and trophic gradient (Turkish Straits System–NE
870 Aegean Sea). *Journal of Marine Systems* 119–120, 1–10.
- 871 Lascaratos, A., Papageorgiou, E., 1987. Flow in the straits of Karpathos (SE. Aegean) during earl y
872 spring' 86. *Terra Cognita*, EGS XII General Assembly, Strasbourg, France, 7 (2–3), 544.
- 873 Le Moigne, Frédéric, A., C., 2019. Pathways of Organic Carbon Downward Transport by the Oceanic
874 Biological Carbon Pump. *Frontiers in Marine Science* 6, 634. doi: 10.3389/fmars.2019.00634.
- 875 Leppäkoski, E., Mihnea, P.E., 1996. Enclosed seas under man-induced change: a comparison between
876 the Baltic and Black Seas. *Ambio* 25, 380–389.
- 877 Lykousis, V., Chronis, G., Tselepidis, A., Price, N.B., Theocharis, A., Siokou-Fragou, I., Wambeke,
878 F.Van, Danovaro, R., Stavrakakis, S., Duineveld, G., Georgopoulos, D., Ignatiades L.,
879 Souvermezoglou, A., Voutsinou-Taliadouri, F., 2002. Major outputs of the recent multidisciplinary
880 biogeochemical researches undertaken in the Aegean Sea. *Journal of Marine Systems* 33–34, 313–
881 334.
- 882 Markaki, Z., Oikonomou, K., Koçak, M., Kouvarakis, G., Chaniotaki, A., Kubilay, N., Mihalopoulos,
883 N., 2003. Atmospheric deposition of inorganic phosphorus in the Levantine Basin, eastern
884 Mediterranean: spatial and temporal variability and its role in seawater productivity. *Limnology and*
885 *Oceanography* 48, 1557–1568.
- 886 Malanotte-Rizzoli, P., Manca, B., Ribera D'Alcala, M., Theocharis, A., Bergamasco, A., Bregant, D.,
887 Budillon, G., Civitarese, G., Georgopoulos, D., Michelato, A., Sansone, E., Scarazzato, P., and
888 Souvermezoglou, E., 1997. A synthesis of the Ionian Sea hydrography, circulation and water mass
889 pathways during POEM-Phase I. *Progress in Oceanography* 39, 153–204.

- 890 Malinverno, E., Karatsolis, B.-Th., Dimiza, M.D., Lagaria, A., Psarra, S., Triantaphyllou, M., 2016.
 891 Extant silicoflagellates from the Northeast Aegean (eastern Mediterranean Sea): Morphologies and
 892 double skeletons. *Revue de Micropaléontologie* 59, 253–265.
- 893 Malinverno, E., Maffioli, P., Corselli, C., De Lange, G., 2014. Present-day fluxes of coccolithophores
 894 and diatoms in the pelagic Ionian Sea. *Journal of Marine Systems* 132, 13–27.
- 895 Malinverno, E., Triantaphyllou, M.V., Stavrakakis, S., Ziveri, P., Lykousis, V., 2009. Seasonal and
 896 spatial variability of coccolithophore export production at the South-Western margin of Crete (Eastern
 897 Mediterranean). *Marine Micropaleontology* 71, 131–147.
- 898 Malinverno, E., Ziveri, P., Corselli, C., 2003. Coccolithophorid distribution in the Ionian Sea and its
 899 relationship to eastern Mediterranean circulation during late fall to early winter 1997. *Journal of*
 900 *Geophysical Research* 108 (C9), 8115.doi:10.1029/2002JC001346.
- 901 McIntyre, A., Bé, A., 1967. Modern coccolithophoridae of the Atlantic ocean-I. Placoliths and
 902 cyrtoliths. *Deep-Sea Research* 14, 561–597.
- 903 Meier, K.J.S., Beaufort, L., Heussner, S., Ziveri, P., 2014. The role of ocean acidification in *Emiliania*
 904 *huxleyi* coccolith thinning in the Mediterranean Sea. *Biogeosciences* 11, 2857–2869.
- 905 Milliman, J.D., 1993. Production and accumulation of calcium carbonate in the ocean: budget of a
 906 non steady state. *Global Biogeochemical Cycles* 7, 927–957.
- 907 Molino, B., McIntyre, A., 1990. Precessional forcing of nutricline dynamics in the equatorial
 908 Atlantic. *Science* 249, 766–769.
- 909 Molinaroli, E., Guerzoni, S., Rampazzo, G., 1993. Contribution of Saharan dust to the central
 910 Mediterranean Basin. *Geological Society of America Spec. Paper* 284, 303–312.
- 911 Moulin, C., Lambert, C.E., Dulac, F., Dayan, U., 1997. Control of atmospheric export of dust from
 912 North Africa by the North Atlantic Oscillation. *Nature* 387, 691–694.
- 913 Nieuwenhuize, J., Maas, Y.E.M., Middelburg, J.J., 1994. Rapid analysis of organic carbon and
 914 nitrogen in particulate materials. *Marine Chemistry* 45, 217–224.
- 915 Nittis, K., Pinardi, N., Lascaratos, A., 1994. Characteristics of the summer 1987 flow field in the
 916 Ionian Sea. *Journal of Geophysical Research* 98, 10171–10184.
- 917 Nowald, N., Karakas, G., Ratmeyer, V., Fischer, G., Schlitzer, R., Davenport, R.A., Wefer, G., 2006.
 918 Distribution and transport processes of marine particulate matter off Cape Blanc (NW-Africa): results
 919 from vertical camera profiles. *Ocean Science Discussions* 3, 903–938.
- 920 Oguz, T., Ducklow, H.W., Malanotte-Rizzoli, P., Murray, J.W., Shushkina, E.A., Vedernikov, V.I.,
 921 Unluata, U., 1999. A physical-biochemical model of plankton productivity and nitrogen cycling in the
 922 Black Sea. *Deep-Sea Research Part I* 46, 597–636.

- 923 Oguz, T., Latun, V.S., Latif, M.A., Vladimirov, V.V., Sur, H.I., Markov, A.A., Özsoy, E.,
 924 Kotovshchikov, B.B., Ereemeev, V.V., Ünlüata, Ü., 1993. Circulation in the surface and intermediate
 925 layers of the Black Sea. *Deep-Sea Research Part I* 40, 1597–1612.
- 926 Oguz, T., Tugrul, S., Kideys, A.E., Ediger, V., Kubilay, N., 2006. Physical and biogeochemical
 927 characteristics of the Black Sea. In: Robinson, A.R., Brink, K.H. (Eds.), *The Sea. The Global Coastal*
 928 *Ocean: Interdisciplinary Regional Studies and Syntheses*, Vol., 14A. Harvard University Press, 1333–
 929 1372.
- 930 Okada, H., Honjo, S., 1973. The distribution of ocean coccolithophorids in the Pacific. *Deep-Sea*
 931 *Research* 20, 355–374.
- 932 Okada, H., McIntyre, A. 1979. Seasonal distribution of modern coccolithophores in the western North
 933 Atlantic Ocean. *Marine Biology* 54, 319–328.
- 934 Okada H., Wells, P., 1997. Late Quaternary nannofossil indicators of climate change in two deep-sea
 935 cores associated with the Leeuwin Current of Western Australia. *Palaeogeography*,
 936 *Palaeoclimatology*, *Palaeoecology* 131, 413–432.
- 937 Patara, L., Pinardi, N., Corselli, C., Malinverno, E., Tonani, M., Santoleri, R., Masina, S., 2009.
 938 Particle fluxes in the deep Eastern Mediterranean basin: the role of ocean vertical velocities.
 939 *Biogeosciences* 6, 333–348.
- 940 Poulos, S.E., Drakopoulos, P.G., Collins, M.B., 1997. Seasonal variability in sea surface
 941 oceanographic conditions in the Aegean Sea (Eastern Mediterranean): an overview. *Journal of Marine*
 942 *Systems* 13, 225–244.
- 943 Psarra, S., Tselepides, A., Ignatiades, L., 2000. Primary productivity in the oligotrophic Cretan Sea
 944 (NE Mediterranean): seasonal and interannual variability. *Progress in Oceanography* 46, 187–204.
- 945 Rembauville, M., Meilland, J., Ziveri, P., Schiebel, R., Blain, S., Salter, I., 2016. Planktic foraminifer
 946 and coccolith contribution to carbonate export fluxes over the central Kerguelen Plateau. *Deep-Sea*
 947 *Research Part I* 111, 91–101.
- 948 Riegman, R., Stolte, W., Noordeloos, A.A.M., 1998. A model system approach to biological climate
 949 forcing: the example of *Emiliana huxleyi*. Final Report Subproject (b): Physiology NIOZ-Rapport
 950 1998-8. Netherlands Institute for Sea Research.
- 951 Rigual-Hernández, A., Trull, T.W., Bray, S.G., Closset, I., Armand, L.K., 2015. Seasonal dynamics in
 952 diatom and particulate export fluxes to the deep sea in the Australian sector of the southern Antarctic
 953 Zone. *Journal of Marine Systems* 142, 62–74.
- 954 Ross, D., Degens, E.T., 1974. Recent sediments of the Black Sea. In: Degens, E.T., and Ross, D.A.
 955 (Eds.), *The Black Sea – Geology, Chemistry and Biology*: Tulsa AAPG, 183–199.

- 956 Rost, B., Riebesell, U., 2004. Coccolithophores and the biological pump: responses to environmental
 957 changes. In: Thierstein, H.R., Young, J.R. (Eds), *Coccolithophores from Molecular Processes to*
 958 *Global Impact*. Springer, Berlin, 99–125.
- 959 Roth, P. H. and Coulbourn, W. T., 1982. Floral and solution patterns of coccoliths in surface
 960 sediments of the North Pacific. *Marine Micropaleontology* 7, 1–52.
- 961 Roussakis, G., Karageorgis, A.P., Conispoliatis, N., Lykousis, V., 2004. Last glacial- Holocene
 962 sediment sequences in N. Aegean basins: structure, accumulation rates and clay mineral distribution.
 963 *Geo-Marine Letters* 24, 97–111.
- 964 Rutten, A., de Lange, G.J., Ziveri, P., Thomson, J., van Santvoort, P.J.M., Colley, S., Corselli C.,
 965 2000. Recent terrestrial and carbonate fluxes in the pelagic eastern Mediterranean; a comparison
 966 between sediment trap and surface sediment. *Palaeogeography, Palaeoclimatology, Palaeoecology*
 967 158, 197–213.
- 968 Saavedra-Pellitero, M., Baumann, K.-H., 2015. Comparison of living and surface sediment
 969 coccolithophore assemblages in the Pacific sector of the Southern Ocean. *Micropaleontology* 61 (6),
 970 507–520.
- 971 Schulz, M., Prospero, J.M., Baker, A.R., Dentener, F., Ickes, L., Liss, P.S., Mahowald, N.M.,
 972 Nickovic, S., Perez García-Pando, C., Rodríguez, S., Sarin, M., Tengen, I., Duce, R.A., 2012.
 973 Atmospheric transport and deposition of mineral dust to the ocean: implications for research needs.
 974 *Environmental Science & Technology* 46, 10390–10404.
- 975 Siokou-Frangou, I., Zervoudaki, S., Christou, E., Zervakis, V., Georgopoulos, D., 2009. Variability of
 976 mesozooplankton spatial distribution in the North Aegean Sea, as influenced by the Black Sea waters
 977 outflow. *Journal of Marine Systems* 78, 557–575.
- 978 Skampa, E., Triantaphyllou, M.V., Dimiza, M.D., Gogou, A., Malinverno, E., Stavrakakis, S.,
 979 Panagiotopoulos, I.P., Parinos, C., Baumann, K.-H., 2019. Coupling plankton-sediment trap-surface
 980 sediment coccolithophore regime in the North Aegean Sea (NE Mediterranean). *Marine*
 981 *Micropaleontology*, doi.org/10.1016/j.marmicro.2019.03.001
- 982 Socal, G., Boldrin, A., Bianchi, F., Civitarese, G., De Lazzari, A., Rabitti, S., Totti, C., Turchetto,
 983 M.M., 1999. Nutrient, particulate matter and phytoplankton variability in the photic layer of the
 984 Otranto Strait. *Journal of Marine Systems* 20, 381–398.
- 985 Sorokin, Y.I., 1983. The Black Sea. In: Kethum, B.H. (Ed.), *Estuaries and Enclosed Seas, Ecosystems*
 986 *of the World*, vol. 26. Elsevier, New York, 253–292.

- 987 Souvermezoglou, E., Krasakopoulou, E., Pavlidou, A., 1999. Temporal variability in oxygen and
 988 nutrients concentrations in the southern Aegean Sea and the straits of the Cretan Arc. *Progress in*
 989 *Oceanography* 44, 573-600.
- 990 Souvermezoglou, E., Krasakopoulou, E., 2002. High oxygen consumption rates in the deep layers of
 991 the north Aegean Sea E. *Mediterranean Marine Science* 3 (1), 55–65.
- 992 Souvermezoglou, E., Krasakopoulou, E., Pavlidou, A., 2014. Temporal and spatial variability of
 993 nutrients and oxygen in the North Aegean Sea during the last thirty years. *Mediterranean Marine*
 994 *Science* 15, 805–822.
- 995 Sprengel, C., Baumann, K.-H., and Neuer, S., 2000. Seasonal and interannual variations in
 996 coccolithophore fluxes and species composition in sediment traps north of Gran Canaria. *Marine*
 997 *Micropaleontology* 49, 3577–3598.
- 998 Stavrakakis, S., Chronis, G., Tselepides, A., Heussner, S., Monaco, A., Abassi, A., 2000. Downward
 999 fluxes of settling particles in the deep Cretan Sea (NE Mediterranean). *Progress in Oceanography* 46,
 1000 217–240.
- 1001 Stavrakakis, S., Gogou, A., Krasakopoulou, E., Karageorgis A., P., Kontoyiannis, H., Rousakis, G.,
 1002 Velaoras, D., Perivoliotis, L., Kambouri, G., Stavrakaki, I., Lykousis, V., 2013. Downward fluxes of
 1003 sinking particulate matter in the deep Ionian Sea (NESTOR site), Eastern Mediterranean: seasonal and
 1004 interannual variability. *Biogeosciences Discussions* 10, 591–641.
- 1005 Sulpis, O., Boudreau, B.P., Mucci, A., Jenkins, C., Trossman, D.S., Arbic, B.K., Key, R.M., 2018.
 1006 Current CaCO_3 dissolution at the seafloor caused by anthropogenic CO_2 . *Proceedings of the National*
 1007 *Academy of Sciences of the United States of America* 115 (46), 11700–11705.
 1008 www.pnas.org/cgi/doi/10.1073/pnas.1804250115
- 1009 Talley, L.D., Pickard, G.L., Emery, W.L., Swift, J.H., 2011. Gravity Waves, Tides, and Coastal
 1010 Oceanography. Chapter 8, In *Descriptive Physical Oceanography*, 6th ed., Swift, J.H., Ed., Academic
 1011 Press: Cambridge, MA, USA, 1–31.
- 1012 Theodosi, C., Markaki, Z., Pantazoglou, F., Tselepides, A., Mihalopoulos, N., 2019. Chemical
 1013 composition of downward fluxes in the Cretan sea (Eastern Mediterranean) and possible link to
 1014 atmospheric deposition: a 7 year survey. *Deep Sea Research Part II*,
 1015 doi.org/10.1016/j.dsr2.2019.06.003.
- 1016 Theocharis A., Georgopoulos, D., Zodiatis, G., and Christianidis, S., 1986. Distribution of the LIW in
 1017 the NW Levantine and SE Aegean. *Proceedings of a UNESCO /IOC workshop on physical*
 1018 *oceanography of the Eastern Mediterranean*. A. R. Robinson and P. Malanotte-Rizzoli, editors. POEM
 1019 scientific report 1, Part 2: Climatology of the Eastern Mediterranean. Cambridge, MA.

- 1020 Triantaphyllou, M.V., 2014. Coccolithophore assemblages during the Holocene climatic optimum in
 1021 the NE Mediterranean (Aegean and northern Levantine Seas, Greece): paleoceanographic and
 1022 paleoclimatic implications. *Quaternary International* 345, 56–67.
- 1023 Triantaphyllou, M.V., Dermitzakis M.D., Dimiza M, 2002. Holo- and Heterococcolithophores
 1024 (calcareous nannoplankton) in the gulf of Korthi (Andros island, Aegean Sea, Greece) during late
 1025 summer 2001. *Revue de Paleobiologie* 21 (1), 353–369.
- 1026 Triantaphyllou, M.V., Karatsolis, B.-T., Dimiza, M.D., Malinverno, E., Cerino, F., Psarra, S., Jordan,
 1027 R.W., Young, J.R., 2015. Coccolithophore combination coccospheres from the NE Mediterranean
 1028 Sea: new evidence and taxonomic revisions. *Micropaleontology* 61 (6), 457–472.
- 1029 Triantaphyllou, M.V., Malinverno, E., Dimiza, M.D., Gogou, A., Athanasiou, A., Skampa, E.,
 1030 Tselenti, D., Thanassoura, E., Birli, A., Stavrakaki, I., Stavrakakis, S., Corselli, C., Lykousis, V.,
 1031 2014. Coccolithophore biogeo-graphic trends and export production in the Eastern Mediterranean and
 1032 BlackSeas. *Journal of Nannoplankton Research* 34, 97–98.
- 1033 Triantaphyllou, M.V., Ziveri, P., Gogou, A., Marino, G., Lykousis, V., Bouloubassi, I., Emeis, K.C.,
 1034 Kouli, K., Dimiza, M., Rosell-Mele, A., Papanikolaou, M., Katsouras, G., Nunez, N., 2009. Late
 1035 Glacial-Holocene climate variability at the south-eastern margin of the Aegean Sea. *Marine Geology*
 1036 266, 182–197.
- 1037 Triantaphyllou, M.V., Ziveri, P., Tselepides, A., 2004. Coccolithophore export production and
 1038 response to seasonal surface water variability in the oligotrophic Cretan Sea (NE Mediterranean).
 1039 *Micropaleontology* 50, 127–144.
- 1040 Tsagaraki, T.M., Herut, B., Rahav, E., Berman Frank, I.R., Tsiola, A., Tsapakis, M., Giannakourou,
 1041 A., Gogou, A., Panagiotopoulos, C., Violaki, K., Psarra, S., Lagaria, A., Christou, E.D.,
 1042 Papageorgiou, N., Zervoudaki, S., Fernandez de Puellas, Ma L., Nikolioudakis, N., Meador, T.B.,
 1043 Tanaka, T., Pedrotti, M.L., Krom, M.D., Paraskevi, P., 2017. Atmospheric Deposition Effects on
 1044 Plankton Communities in the Eastern Mediterranean: A Mesocosm Experimental Approach. *Frontiers*
 1045 *in Marine Science*, doi.org/10.3389/fmars.2017.00210.
- 1046 Tselepides, A., A., Zervakis, V., Polychronaki, T., Danovaro, R., Chronis, G., 2000. Distribution of
 1047 nutrients and particulate organic matter in relation to the prevailing hydrographic features of the
 1048 Cretan Sea (NE Mediterranean). *Progress in Oceanography* 46, 113–142.
- 1049 Tyrrell, T., Taylor, A.H., 1996. A modelling study of *Emiliania huxleyi* in the NE Atlantic. *Journal of*
 1050 *Marine Systems* 9, 83–112.
- 1051 Van der Jagt, H., Friese, C., Stuut, J.-B., W., Fischer, G., Iversen, M. H., 2018. The ballasting effect
 1052 of Saharan dust deposition on aggregate dynamics and carbon export: aggregation, settling and
 1053 scavenging of marine snow. *Limnology and Oceanography* 63, 1386–1394.

- 1054 Velaoras, D., Krokos, G., Nittis, K., Theocharis, A., 2014. Dense intermediate water outflow from the
1055 Cretan Sea: A salinity driven, recurrent phenomenon, connected to thermohaline circulation changes,
1056 Journal of Geophysical Research: Oceans 119, 4797–4820.
- 1057 Wells, P., Okada, H., 1997. Response of nanoplankton to major changes in sea-surface temperature
1058 and movements of hydrological fronts over Site DSDP 594 (south Chatham Rise, south eastern New
1059 Zealand), during the last 130 kyr. Marine Micropaleontology 32, 341–363.
- 1060 Westbroek, P., Brown, C.W., Van Bleijswijk, J., Brownlee, C., Brummer, G.J., Conte, M., Egge, J.,
1061 Fernandez, E., Jordan, R., Knappertsbusch, M., Stefels, J., Veldhuis, M., Van der Wal, P., Young,
1062 J., 1993. A model system approach to biological climate forcing: the example of *Emiliania huxleyi*.
1063 Global and Planetary Change 8, 27–46.
- 1064 Winter, A., Jordan, R.W., Roth, P.H., 1994. Biogeography of living Coccolithophores in ocean
1065 waters. In: Winter, A., Siesser, W.G. (Eds.), Coccolithophores. Cambridge University Press,
1066 Cambridge, UK, 161–178.
- 1067 Young, J.R., Poulton, A.J., Tyrrell, T., 2014. Morphology of *Emiliania huxleyi* coccoliths on the
1068 northwestern European shelf – is there an influence of carbonate chemistry? Biogeosciences 11,
1069 4771–4782.
- 1070 Young, J.R., Ziveri, P., 2000. Calculation of coccolith volume and its use in calibration of carbonate
1071 flux estimates. Deep-Sea Research Part II, 47, 1679–1700.
- 1072 Zervakis, V., Georgopoulos, D., Karageorgis, A.P., Theocharis, A., 2004. On the response of the
1073 Aegean Sea to climatic variability: a review. International Journal of Climatology 24, 1845–1858.
- 1074 Zervakis, V., Georgopoulos, D., Drakopoulos, P.G., 2000. The role of the North Aegean in triggering
1075 the recent Eastern Mediterranean climatic changes. Journal of Geophysical Research: Oceans 105,
1076 26103–26116.
- 1077 Zervoudaki, S., Christou, E.D., Assimakopoulou, G., Örek, H., Gucu, A.C., Giannakourou, A., Pitta,
1078 P., Terbiyik, T., Yücel, N., Moutsopoulos, T., Pagou, K., Psarra, S., Özsoy, E., Papathanassiou, E.,
1079 2011. Copepod communities, production and grazing in the Turkish Straits System and the adjacent
1080 northern Aegean Sea during spring. Journal of Marine Systems 86, 45–56.
- 1081 Ziveri, P., Baumann, K.-H., Boeckel, B., Bollmann, J., Young, J.R., 2004. Biogeography of selected
1082 holocene coccoliths in the Atlantic Ocean. In: Thierstein, H.R., Young, J.R. (Eds.), Coccolithophores-
1083 From Molecular Processes to Global Impact. Springer-Verlag, 403–428.
- 1084 Ziveri, P., de Bernardi, B., Baumann, K.H., Stolle, H.M., Mortyn, P.G., 2007. Sinking of coccolith
1085 carbonate and potential contribution to organic carbon ballasting in the deep ocean. Deep-Sea
1086 Research Part II 54, 659–675.

- 1087 Ziveri, P., Grandi, C., Stefanetti, A., 1995. Biogenic fluxes in Bannock Basin: first results from a
1088 sediment trap study (November 1991-May 1992). *Rendiconti Fisici Accademia Lincei* 9, 6, 131–145.
- 1089 Ziveri, P., Broerse, A.T.C., Van Hinte, J. E., Westroek, P., Honjo, S. 2000a. The fate of coccoliths at
1090 48°N21°W, northeastern Atlantic. *Deep Sea Research II* 47, 1853–1875.
- 1091 Ziveri, P., Rutten, A., de Lange, G. J., Thomson, J., Corselli, C. 2000b. Present-day coccolith fluxes
1092 recorded in central eastern Mediterranean sediment traps and surface sediments. *Palaeogeography,*
1093 *Palaeoclimatology, Paleoecology* 158(3–4), 175–195.
- 1094 Ziveri, P., Young, J.R., Van Hinte, J.E., 1999. Coccolithophore export production and accumulation
1095 rates. *GeoResearch Forum* 5, 41–56.

FIGURE CAPTIONS

Fig. 1. (a) Geographical location of the study areas (i.e., Black Sea, North Aegean, Cretan Sea, Ionian Sea) and time-series sediment traps (see red bullets). **(b)** Main patterns of the surface water mass circulation (BSW: Black Sea Water; LW: Levantine Water; MAW; Modified Atlantic Water)

Fig. 2. Physico-chemical components of the flux concerning the study areas: **(a)** North Aegean Sea; **(b)** Cretan Sea; **(c)** Ionian Sea **(d)** Black Sea. Data have been estimated from the sediment trap datasets.

Fig. 3. (a) Total coccolith and coccosphere fluxes and major species coccolith and coccosphere fluxes. **(b)** Total minor species coccolith flux (including coccosphere units converted to coccolith numbers according to Boeckel and Baumann, 2008) and major vs. minor species relative abundances in the North Aegean Sea.

Fig. 4. (a) Total coccolith and coccosphere fluxes and major species coccolith and coccosphere fluxes. **(b)** Total minor species coccolith flux (including coccosphere units converted to coccolith numbers according to Boeckel and Baumann, 2008) and major vs. minor species relative abundances in the Cretan Sea

Fig. 5. (a) Total coccolith and coccosphere fluxes and major species coccolith and coccosphere fluxes. **(b)** Total minor species coccolith flux (including coccosphere units converted to coccolith numbers according to Boeckel and Baumann, 2008) and major vs. minor species relative abundances in the Ionian Sea

Fig. 6. (a) Total coccosphere flux and *E. huxleyi* and *Syracosphaera* spp. coccosphere fluxes in the Black Sea. **(b)** Total coccosphere units have been converted to coccolith numbers according to Boeckel and Baumann (2008)

Fig. 7. Total coccolith flux (including coccosphere units converted to coccolith numbers according to Boeckel and Baumann, 2008), species relative abundances and average relative abundances for the entire investigated time interval **(a)** North Aegean Sea; **(b)** Cretan Sea; **(c)** Ionian Sea.

Fig. 8. Relative mass contribution from different species in: **(a)** North Aegean Sea; **(b)** Cretan Sea; **(c)** Ionian Sea. *Emiliania huxleyi* coccolith mass is calculated by own estimations according to morphometric analyses (Supplementary Appendix 1) applied to the equation of Young and Ziveri (2000).

Fig. 9. Total coccolith fluxes (including coccosphere units converted to coccolith numbers according to Boeckel and Baumann, 2008) in the three investigated areas during cold (November-April) and warm (May-October) time spans in 2015.

TABLE CAPTIONS

Table 1. Sediment trap deployments, Black Sea, North Aegean Sea, Cretan Sea, Ionian Sea. Mooring stations, trap depths and water column depths.

Table 2. Sampling details of the four investigated sediment trap mooring sites; Black Sea, North Aegean Sea, Cretan Sea and Ionian Sea

Table 3. Identification criteria for the major sea water masses in the Black, Aegean and Ionian Seas (Nittis et al., 1993; Oguz et al., 1993; Malanotte-Rizzoli et al., 1997; Zervakis et al., 2000; Lykousis et al., 2002; Talley et al., 2011; Velaoras et al., 2014)

Table 4. Mean number of coccoliths per coccosphere for the most abundant coccosphere species used in this study, mainly based on Boeckel and Baumann (2008).

Table 5. Coccolith masses of the main individual species, mainly based on Young and Ziveri (2000), Baumann (2004).

**Emiliana huxleyi* mass is estimated on a monthly basis from the available sampling material and average mass values are provided for the intervals May-October and November-April. Calculations are based on coccolith size parameters measured in the North Aegean, Cretan and Ionian sampling series (Supplementary Appendix 1).

Table 6. Correlation matrix (Spearman) among coccolithophore fluxes and physico-chemical components of the flux. R values greater than |0.238| are significant with 95% probability.

Supplementary Fig. 1. Satellite-derived data concerning the study areas: (a) Black Sea (the relevant information have been derived only via the processing of the sediment trap time series); (b) North Aegean Sea; (c) Cretan Sea; (d) Ionian Sea.: SST, chlorophyll-a and precipitation variations during the studied time interval have been derived from satellite data obtained from <http://disc.sci.gsfc.nasa.gov/techlab/giovanni/> (all analyses and visualizations of this study were produced with the Giovanni online data system, developed and maintained by the NASA GES DISC).

Supplementary Appendix 1: *Emiliana huxleyi* coccolith morphometric measurements (according to Young et al., 2014) and coccolith mass calculations, based on the equation of Young and Ziveri (2000).

Supplementary Appendix 2: Coccolithophore taxa fluxes and relative abundances in each investigated site.

Black Sea			North Aegean Sea			Cretan Sea			Ionian Sea		
Sample code	Start sampling date	Sampling duration (days)	Sample code	Start sampling date	Sampling duration (days)	Sample code	Start sampling date	Sampling duration (days)	Sample code	Start sampling date	Sampling duration (days)
STRAPIA1	16/10/07	16	AM2-A1	13/01/2011	19	PTIV1B1	16/01/2001	15	KMSIXC2	16/06/2010	15
STRAPIA2	1/11/07	15	AM2-A2	01/02/2011	15	PTIV1B2	01/02/2001	15	KMSXC5	16/01/2011	16
STRAPIA3	16/11/07	15	AM2-A3	15/02/2011	14	PTIV1B3	16/02/2001	13	KMSXC6	01/02/2011	15
STRAPIA4	1/12/07	15	AM2-A6	01/04/2011	15	PTIV1B4	01/03/2001	15	KMSXC7	16/02/2011	13
STRAPIA5	16/12/07	16	AM3-A1	07/05/2011	25	PTIV1B5	16/03/2001	16	KMSXC8	01/03/2011	15
STRAPIA6	1/01/08	15	AM3-A2	01/06/2011	15	PTIV1B6	01/04/2001	15	KMSXC10	01/04/2011	15
STRAPIA7	16/01/08	16	AM3-A3	16/06/2011	15	PTIV1B7	16/04/2001	15	KMSXC11	15/04/2011	16
STRAPIA8	1/02/08	15	AM3-A4	01/07/2011	15	PTIV1B8	01/05/2001	15	KMSXC12	15/05/2011	15
STRAPIA9	16/02/08	14	AM3-A5	16/07/2011	16	PTIV1B9	16/05/2001	16	KMSXIC2	01/06/2011	15
STRAPIA10	1/03/08	15	AM3-A6	01/08/2011	31	PTIV1B10	01/06/2001	15	KMSXIC9	11/10/2011	31
STRAPIA11	16/03/08	16	AM3-A7	01/09/2011	30	PTIV1B11	16/06/2001	15	KMSXIC1	01/03/2012	15
STRAPIIA1	16/04/08	15	AM3-A9	01/11/2011	15	PTIV1B12	01/07/2001	15	KMSXIC2	16/03/2012	16
STRAPIIA2	1/05/08	15	AM3-A10	16/11/2011	15	PTV1B1	16/08/2001	16	KMSXIC3	01/04/2012	15
STRAPIIA3	16/05/08	16	AM3-A11	01/12/2011	15	PTV1B2	01/09/2001	15	KMSXIC4	16/04/2012	15
STRAPIIA4	1/06/08	15	AM3-A12	16/12/2011	16	PTV1B3	16/09/2001	15	KMSXIC5	01/05/2012	15
STRAPIIA5	16/06/08	15	M2IA1	16/10/2014	16	PTV1B4	01/10/2001	15	KMSXIC6	16/05/2012	16
STRAPIIA6	1/07/08	15	M2IA2	01/11/2014	15	PTV1B5	16/10/2001	16	KMSXIC8	16/06/2012	15
STRAPIIA7	16/07/08	16	M2IA3	16/11/2014	15	PTV1B6	01/11/2001	15	KMSXIC9	01/07/2012	15
STRAPIIA8	1/08/08	15	M2IA4	01/12/2014	15	PTV1B7	16/11/2001	15	KMSXIC10	16/07/2012	16
STRAPIIA10	1/09/08	15	M2IA5	16/12/2014	16	PTV1B8	01/12/2001	15	KMSXIC11	01/08/2012	15
STRAPIIA11	16/09/08	15	M2IA6	01/01/2015	15	PTV1B9	16/12/2001	16	KMSXIC12	16/08/2012	16
			M2IA7	16/01/2015	16	PTV1B10	01/01/2002	15	KMSXVC1	16/10/2014	16
			M2IA8	01/02/2015	15	PTV1B11	16/01/2002	16	KMSXVC3	16/11/2014	15
			M2IA9	16/02/2015	13	PTV1B12	01/02/2002	15	KMSXVC4	01/12/2014	15
			M2IA11	16/03/2015	16	M3AVIIB6	01/01/2015	16	KMSXVC5	16/12/2014	16

Table 2. Sampling details of the four investigated sediment trap mooring sites; Black Sea, North Aegean Sea, Cretan Sea and Ionian Sea

Black Sea			North Aegean Sea			Cretan Sea			Ionian Sea		
Sample code	Start sampling date	Sampling duration (days)	Sample code	Start sampling date	Sampling duration (days)	Sample code	Start sampling date	Sampling duration (days)	Sample code	Start sampling date	Sampling duration (days)
			M2IA12	01/04/2015	15	M3AVIIB7	15/01/2015	15	KMSXVC6	01/01/2015	15
			M2IIA1	01/06/2015	15	M3AVIIB8	01/02/2015	16	KMSXVC7	16/01/2015	16
			M2IIA2	16/06/2015	15	M3AVIIB9	15/02/2015	15	KMSXVC8	01/02/2015	15
			M2IIA3	01/07/2015	15	M3AVIIB10	01/03/2015	16	KMSXVC9	16/02/2015	13
			M2IIA4	16/07/2015	16	M3AVIIB11	15/03/2015	15	KMSXVC11	16/03/2015	16
			M2IIA5	01/08/2015	15	M3AVIIB12	01/04/2015	16	KMSXVC12	01/04/2015	15
			M2IIA7	01/09/2015	15	M3AVIIB1	01/08/2015	15	KMSXVIC1	01/06/2015	15
			M2IIA8	16/09/2015	15	M3AVIIB2	16/08/2015	16	KMSXVIC2	16/06/2015	15
			M2IIA9	01/10/2015	15	M3AVIIB3	01/09/2015	15	KMSXVIC3	01/07/2015	15
			M2IIA10	16/10/2015	15	M3AVIIB4	16/09/2015	15	KMSXVIC4	16/07/2015	16
			M2IIA11	01/11/2015	15	M3AVIIB5	01/10/2015	15	KMSXVIC5	01/08/2015	15
						M3AVIIB6	16/10/2015	16	KMSXVIC7	01/09/2015	15
						M3AVIIB7	01/11/2015	15			
						M3AVIIB8	16/11/2015	15			
						M3AVIIB10	16/12/2015	15			

Table 2 (Continued)

Location	Water mass	Depth (m)	Temperature (°C)	Salinity (psu)	Description
Black Sea (Oguz et al., 1993; Talley et al., 2011)	Cold Intermediate Layer	~100	<8	~20	Fresh, temperature minimum
	Deep Waters		~8.9	~22.3	warm, salty
North Aegean Sea (Zervakis et al., 2000; Lykousis et al., 2002)	Black Sea Waters	<70		24-28	fresh
	Levantine Surface Waters			>39	warm, salty
	Levantine Intermediate Waters	100-400	14-15	38.8-39.1	warm, salty
	North Aegean Deep Waters				very dense
Cretan Sea (Velaoras et al., 2014)	Modified Atlantic Waters	<100		38.5-38.9	Salinity minimum
	Black Sea Waters			<38.9	
	Levantine Surface Waters	<50		>39.3	salty
	Levantine Intermediate Waters	100-400		38.9-39.1	warm, salty
	Cretan Deep Waters	>800		~39.08	oxygenated
Ionian Sea (Nittis et al., 1993; Malanotte-Rizzoli et al., 1997)	Modified Atlantic Waters	25-100	15-17	~38.7	salinity minimum
	Levantine Intermediate Waters	100-500	14-15	38.8-39	salinity maximum
	Transitional Waters	500-1200	13-14	~38.7	properties intermediate between LIW and EMDW
	Eastern Mediterranean Deep Waters	>1200	~13	~38.6	cold, less saline

Table 3. Identification criteria for the major sea water masses in the Black, Aegean and Ionian Seas (Nittis et al., 1993; Oguz et al., 1993; Malanotte-Rizzoli et al., 1997; Zervakis et al., 2000; Lykousis et al., 2002; Talley et al., 2011; Velaoras et al., 2014)

Species	Mass at mean length (pg)
<i>A. robusta</i>	180.0
<i>C. leptoporus</i>	74.1
<i>E. huxleyi</i>	*2.8 (May-October) *3.0 (November- April)
<i>H. carteri</i>	135.0
<i>Pontosphaera</i> spp.	540.0
<i>R. clavigera</i>	67.5
<i>S. mediterranea</i>	12.1
<i>S. pulchra</i>	13.5
<i>U. sibogae</i>	16.9
<i>U. tenuis</i>	8.7

Table 5. Coccolith masses of the main individual species, mainly based on Young and Ziveri (2000), Baumann (2004).

**Emiliana huxleyi* mass is estimated on a monthly basis from the available sampling material and average mass values are provided for the intervals May-October and November-April. Calculations are based on coccolith size parameters measured in the North Aegean, Cretan and Ionian sampling series (Appendix 1).

Correlation matrix (Spearman)

			Total Mass flux	CaCO ₃ flux	Total Organic Carbon flux	Total coccolithophore Carbonate flux	Lithogenic flux	PIC flux	Total coccosphere flux	<i>E. huxleyi</i> coccosphere flux	<i>E. huxleyi</i> coccolith flux	<i>E. huxleyi</i> flux (coccoliths including coccosphere converted to coccoliths)	<i>F. profunda</i> coccolith flux
Spearman's rho	Total Mass flux	Correlation Coefficient	1.000	,550**	,861**	,228*	,663**	,812**	,592**	,703**	,675**	,677**	,647**
		Sig. (2- tailed)		.000	.000	.035	.000	.000	.000	.000	.000	.000	.000
		N	129	129	129	86	72	71	120	104	109	105	109
	CaCO ₃ flux	Correlation Coefficient	,550**	1.000	,495**	,327**	,865**	1,000**	,524**	,537**	,513**	,529**	,566**
		Sig. (2- tailed)	.000		.000	.002	.000		.000	.000	.000	.000	.000
		N	129	129	129	86	72	71	120	104	109	105	109
	Total Organic Carbon flux	Correlation Coefficient	,861**	,495**	1.000	-.040	,690**	,549**	,691**	,717**	,640**	,641**	,672**
		Sig. (2- tailed)	.000	.000		.716	.000	.000	.000	.000	.000	.000	.000
		N	129	129	129	86	72	71	120	104	109	105	109
	Total coccolithophore Carbonate flux	Correlation Coefficient	,228*	,327**	-.040	1.000	,363*	,501**	.044	,335**	,628**	,700**	,342**
		Sig. (2- tailed)	.035	.002	.716		.035	.000	.696	.006	.000	.000	.004
		N	86	86	86	86	34	49	82	66	71	67	71
	Lithogenic flux	Correlation Coefficient	,663**	,865**	,690**	,363*	1.000	,800**	,491**	,482**	,751**	,730**	,784**
		Sig. (2- tailed)	.000	.000	.000	.035		.000	.000	.000	.000	.000	.000
		N	72	72	72	34	72	51	72	71	72	72	72
	PIC flux	Correlation Coefficient	,812**	1,000**	,549**	,501**	,800**	1.000	,373**	,712**	,533**	,614**	,471**
		Sig. (2- tailed)	.000		.000	.000	.000		.002	.000	.000	.000	.000
		N	71	71	71	49	51	71	66	50	51	51	51

** Correlation is significant at the 0.01 level (2-tailed).

* Correlation is significant at the 0.05 level (2-tailed).

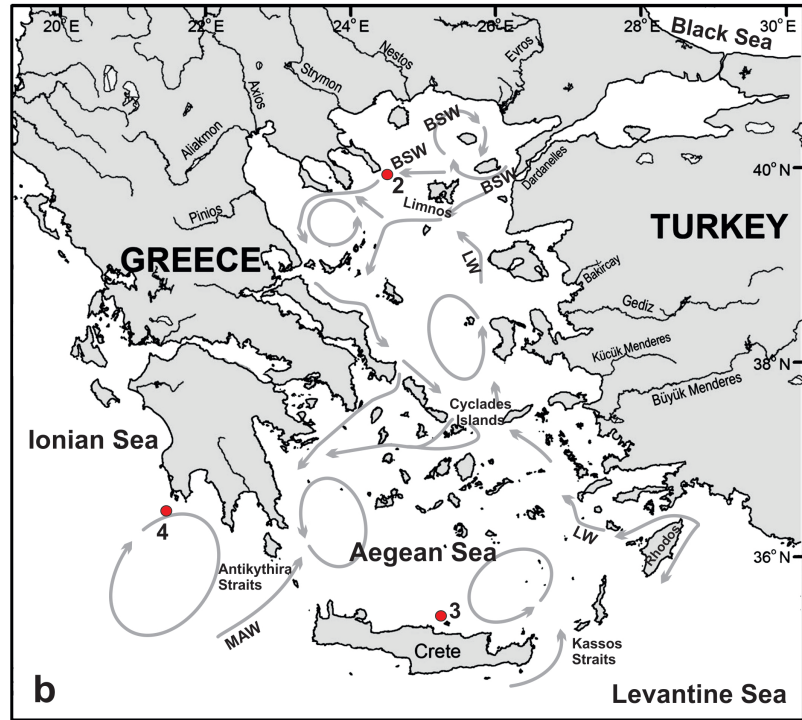
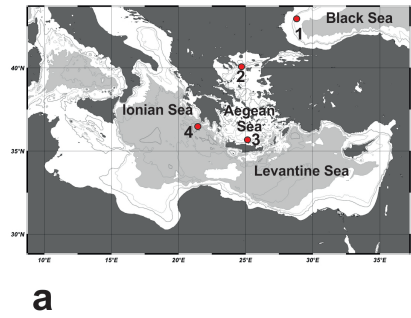
Table 6. Correlation matrix (Spearman) among coccolithophore fluxes and physico-chemical components of the flux. R values greater than |0.238| are significant with 95% probability.

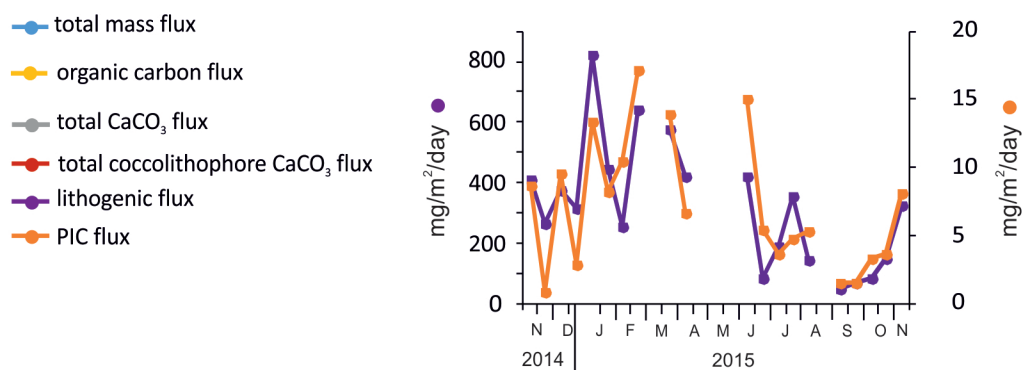
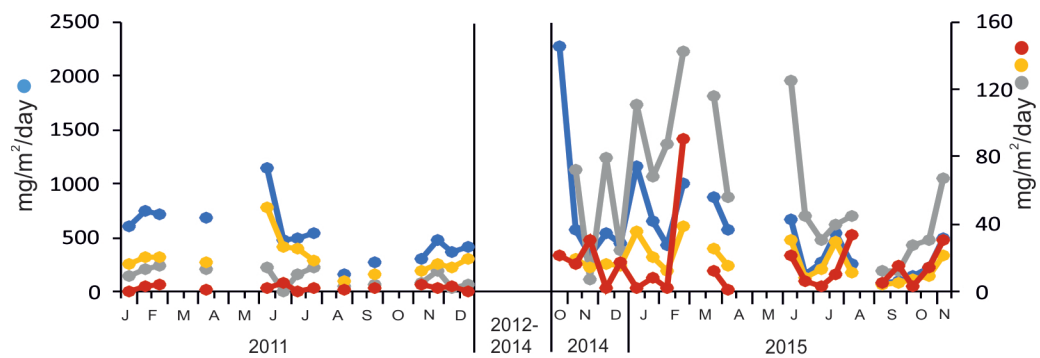
Sediment trap code name, mooring location	BS Black Sea	M2-Athos basin North Aegean Sea	M3 Cretan Sea		Nestor site SE Ionian Sea
Investigated interval	2007-08	2011, 2014-15	2001-02	2015	2011-12, 2014-15
Coordinates	42°58.00'N 29°29.00'E	39°58.16'N 24°43.48'E	35°48.6'N 25°06.6'E	35°44.76'N 25°09.29'E	36°2.96' N 21°28.93' E
Mooring depth (m)	965	500	1700	1470	2000
Water column depth (m)	2000	970	1750	1570	4500

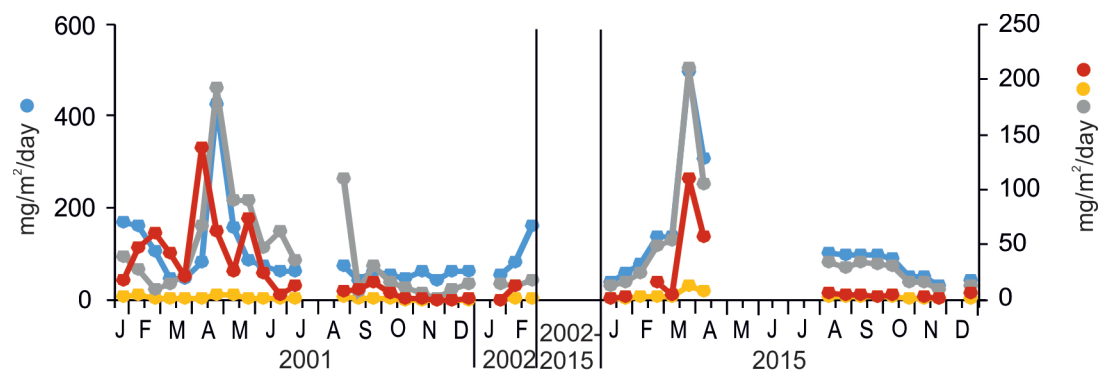
Table 1. Sediment trap deployments, Black Sea, North Aegean Sea, Cretan Sea, Ionian Sea. Mooring stations, trap depths and water column depths.

Species	Mean coccoliths per coccosphere
<i>A. robusta</i>	32
<i>C. leptoporus</i>	29
<i>C. brasiliensis</i>	120
<i>D. tubifera</i>	47
<i>E. huxleyi</i>	24
<i>H. carteri</i>	21
<i>Pontosphaera</i> spp.	38
<i>R. clavigera</i>	27
<i>R. xiphos</i>	38
<i>S. mediterranea</i>	43
<i>S. pulchra</i>	45
<i>U. sibogae</i>	68
<i>U. tenuis</i>	25

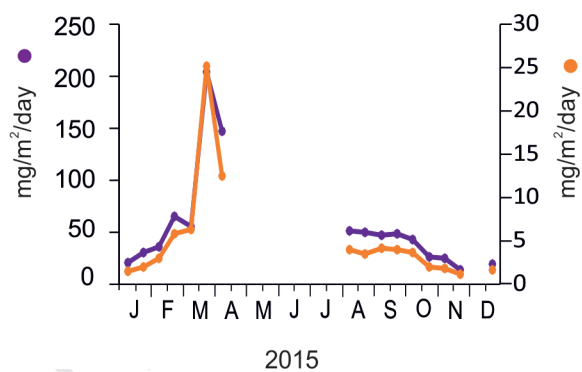
Table 4. Mean number of coccoliths per coccosphere for the most abundant coccosphere species used in this study, mainly based on Boeckel and Baumann (2008).

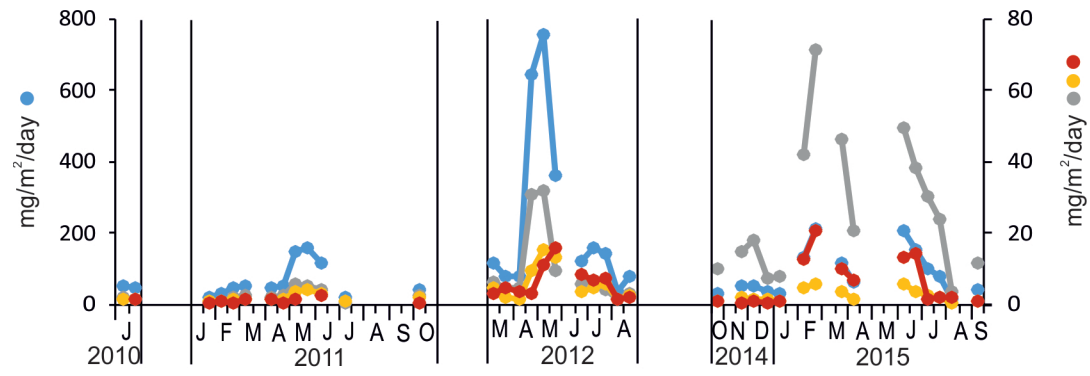




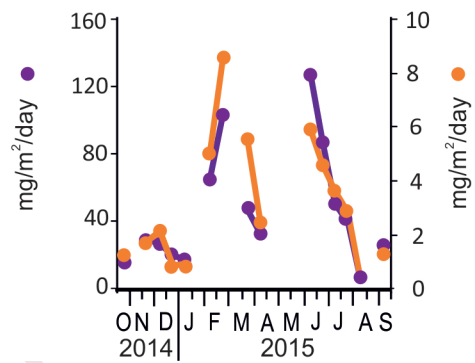


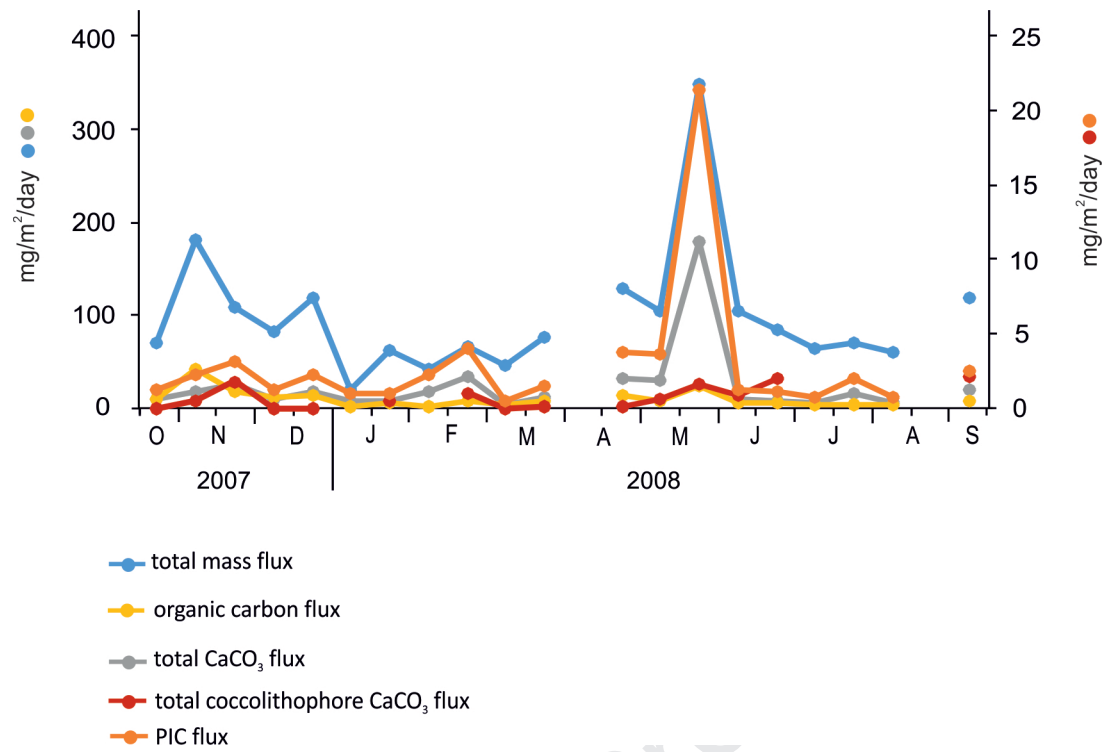
- total mass flux
- organic carbon flux
- total CaCO_3 flux
- total coccolithophore CaCO_3 flux
- lithogenic flux
- PIC flux

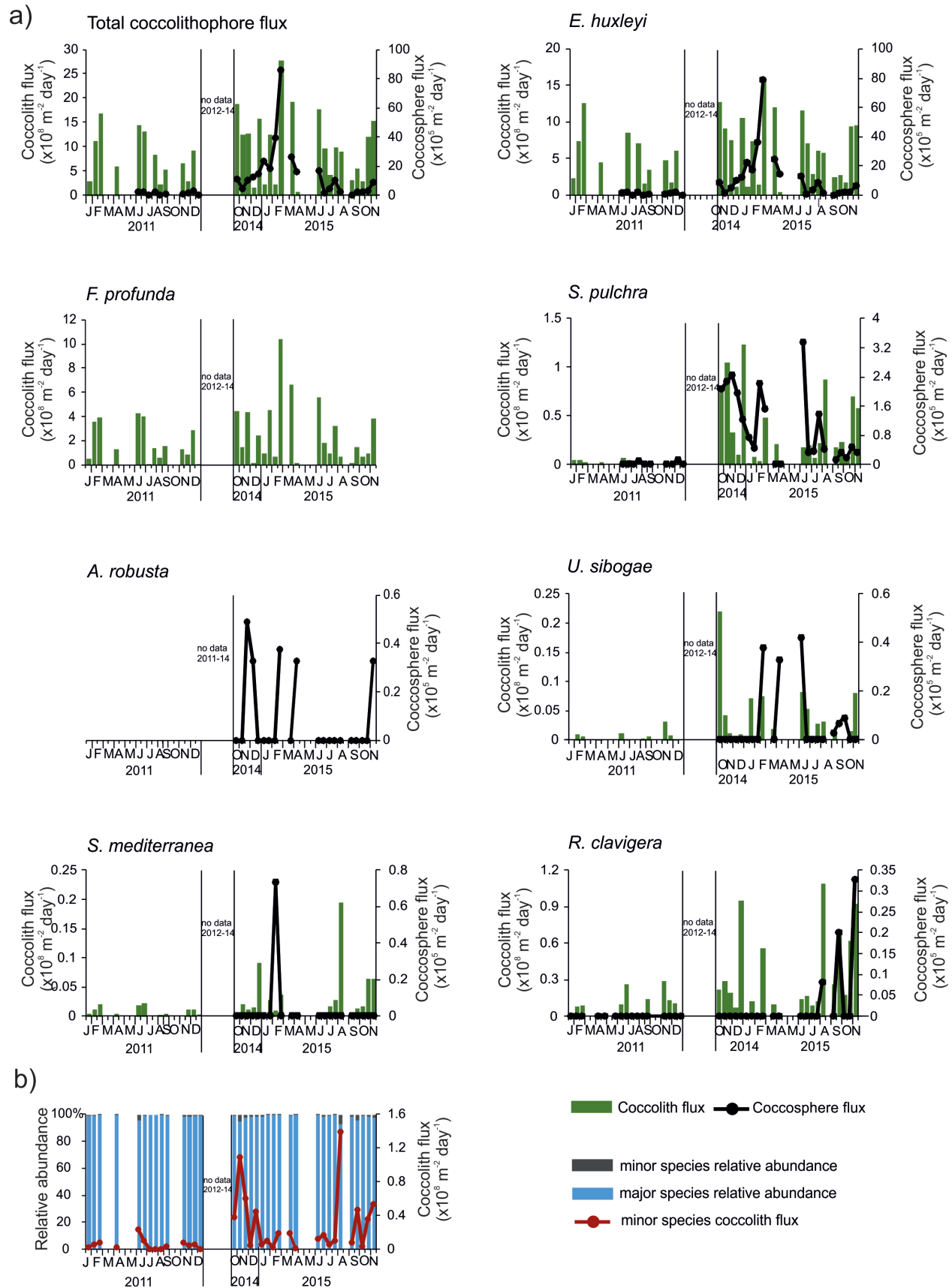




- total mass flux
- organic carbon flux
- total CaCO₃ flux
- total coccolithophore CaCO₃ flux
- lithogenic flux
- PIC flux

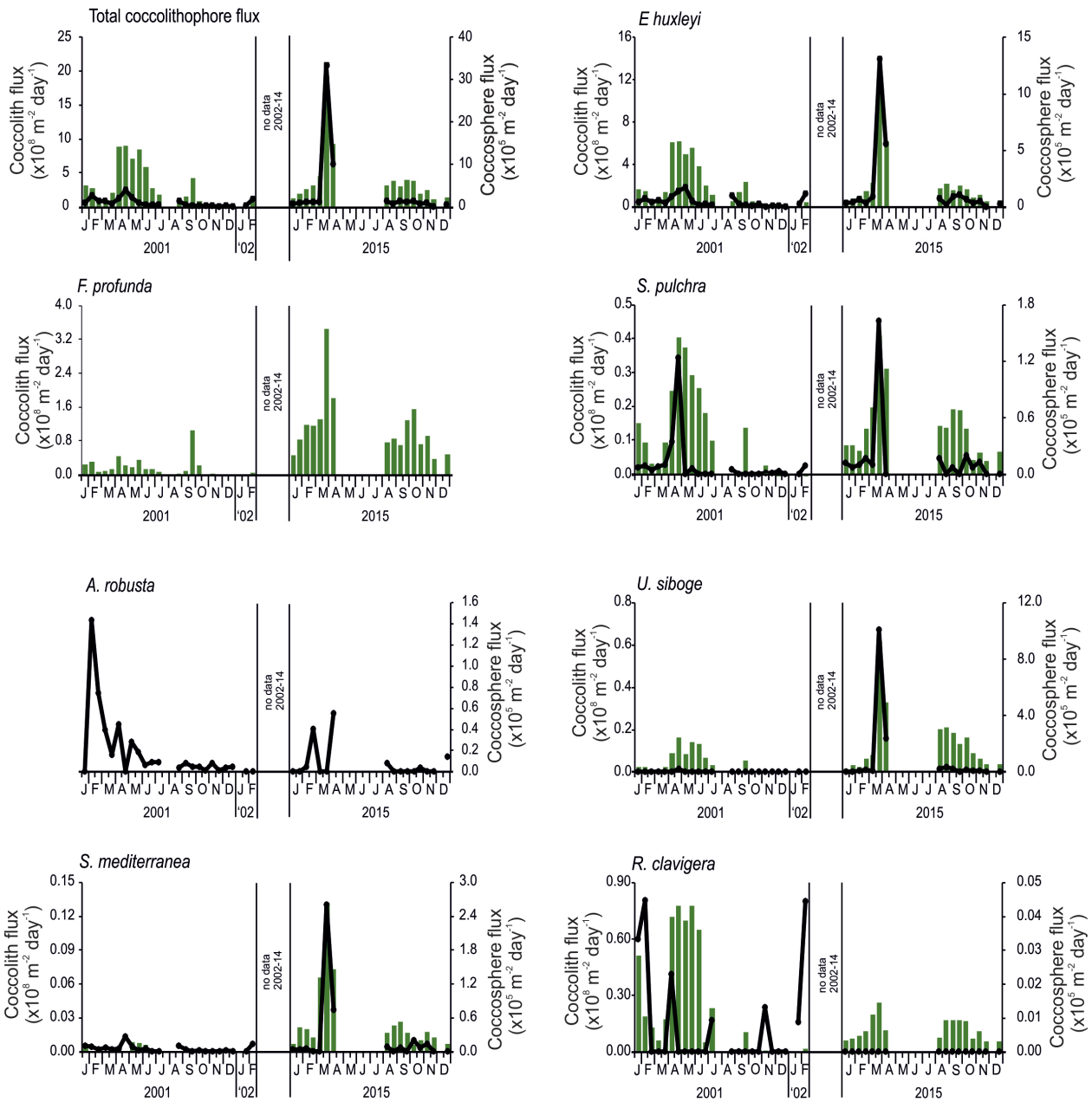




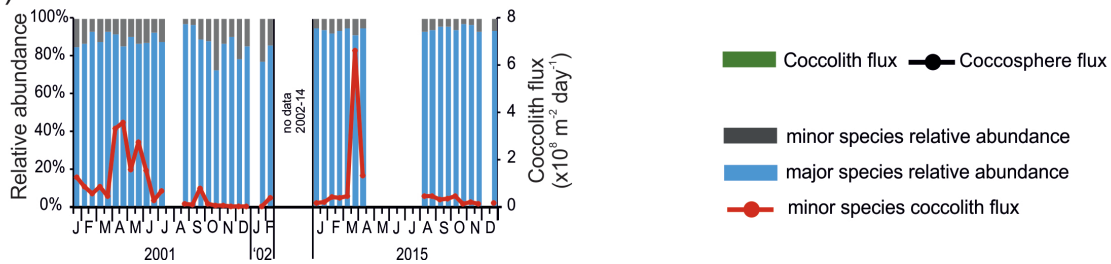


Journal Pre-proof

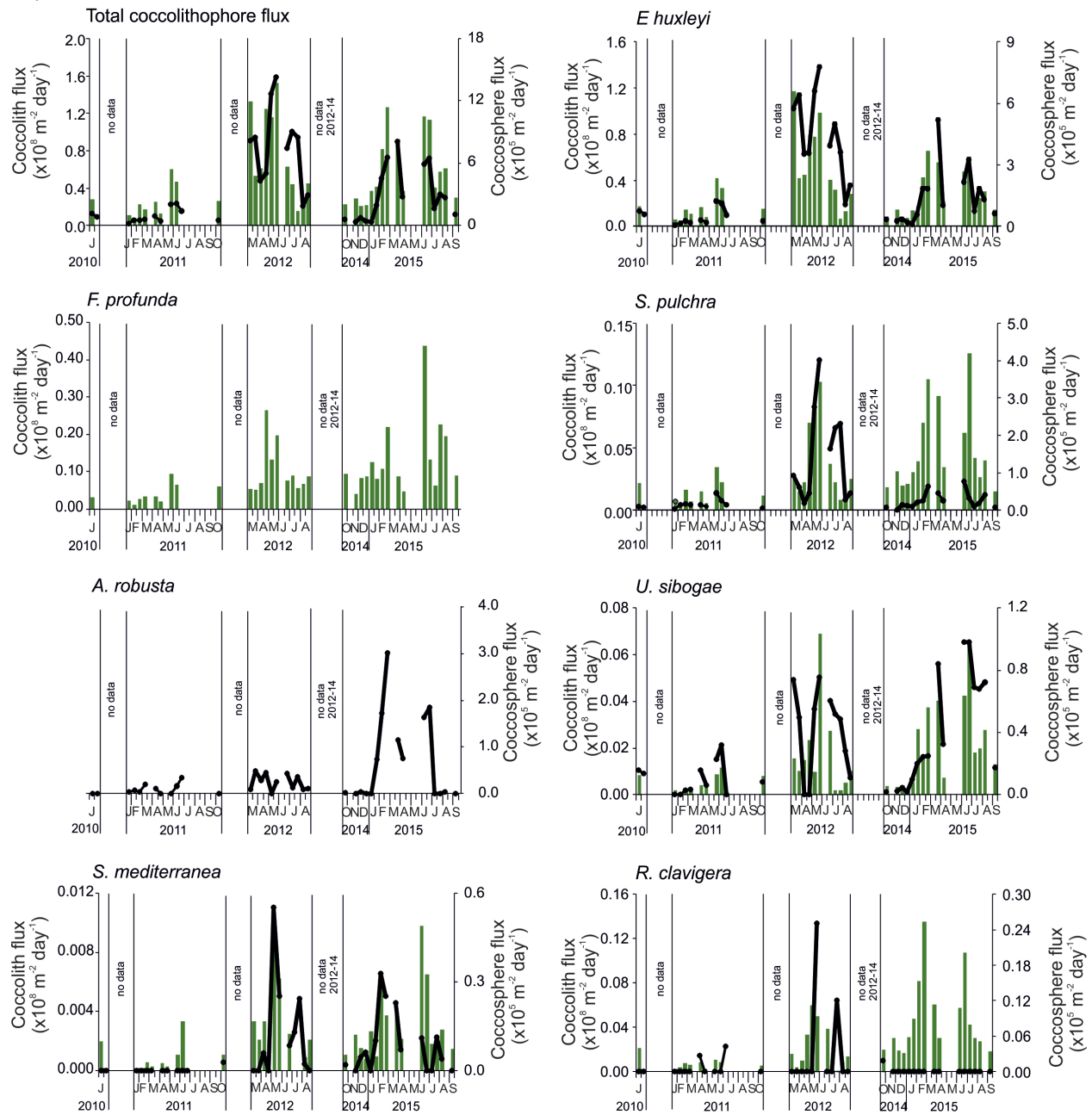
a)



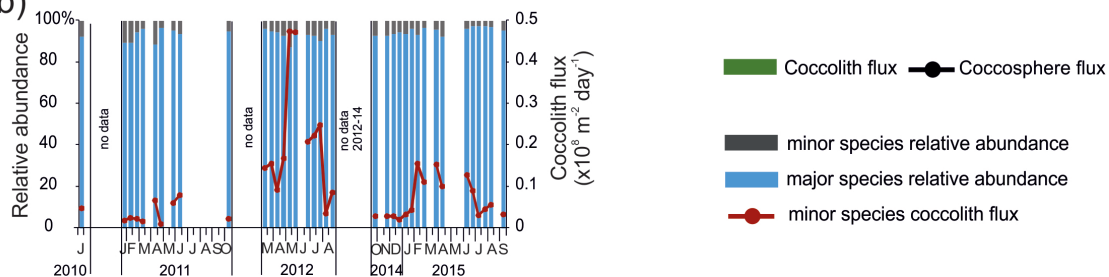
b)



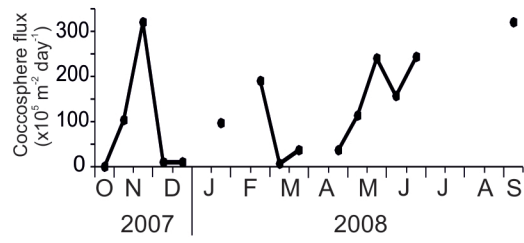
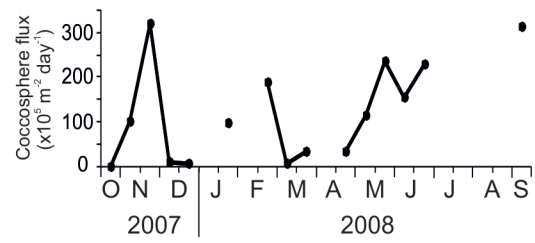
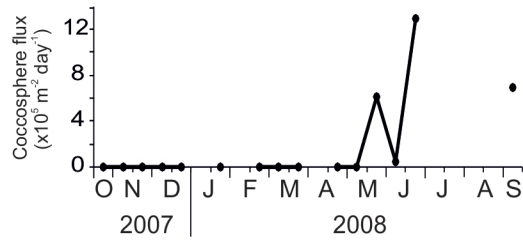
a)



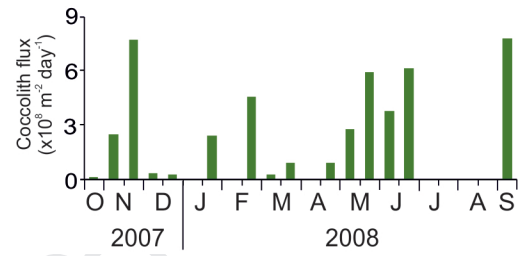
b)



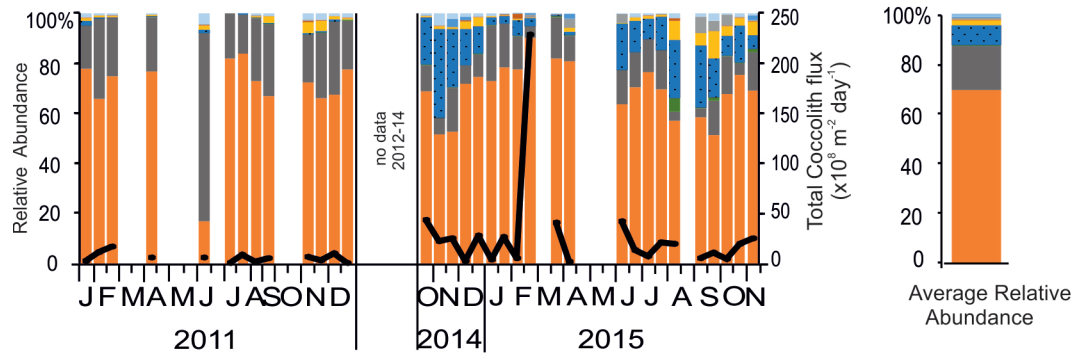
a) Total coccosphere flux

*E. huxleyi**Syracosphaera dilatata*

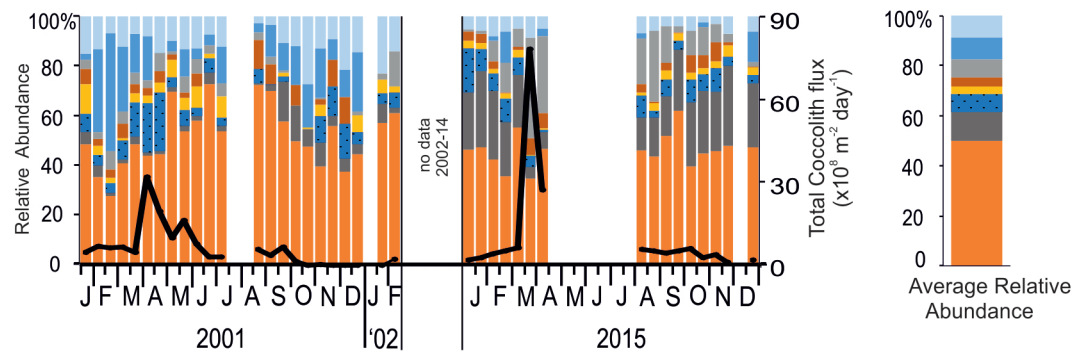
b) Total coccolith flux (total coccosphere countings converted to coccoliths)



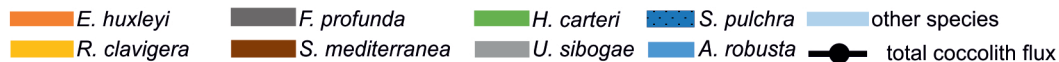
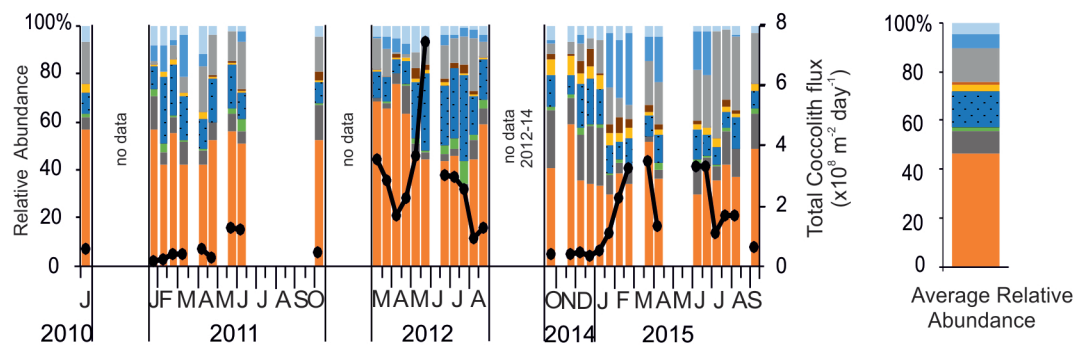
a) North Aegean Sea



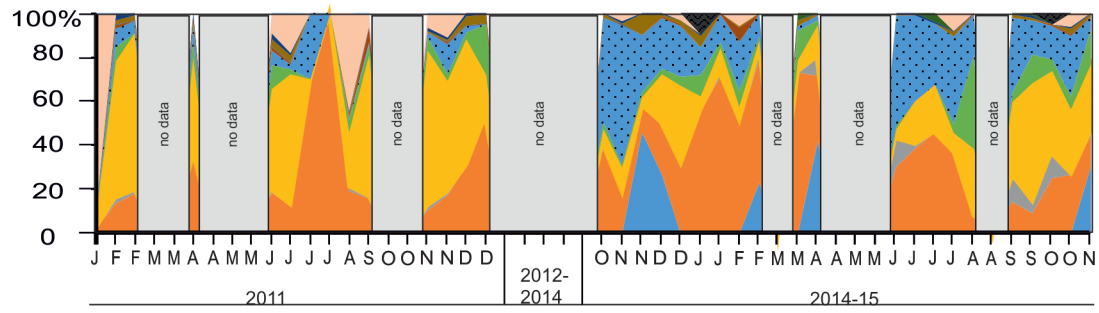
b) Cretan Sea



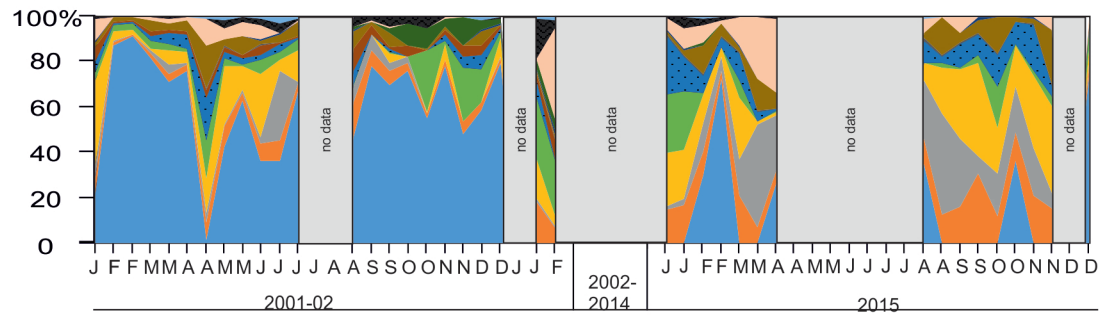
c) Ionian Sea



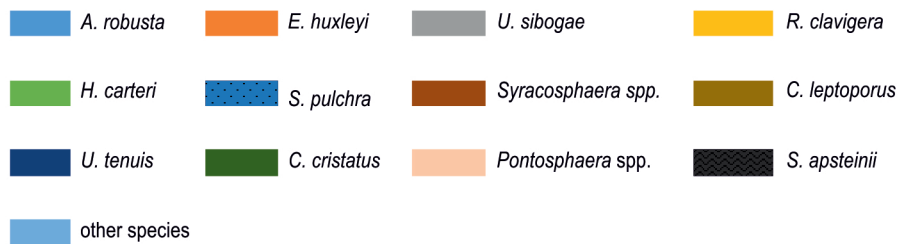
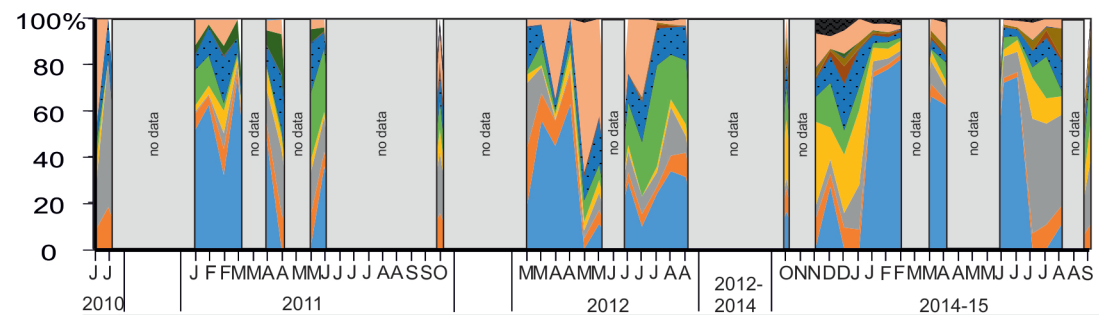
a) North Aegean Sea

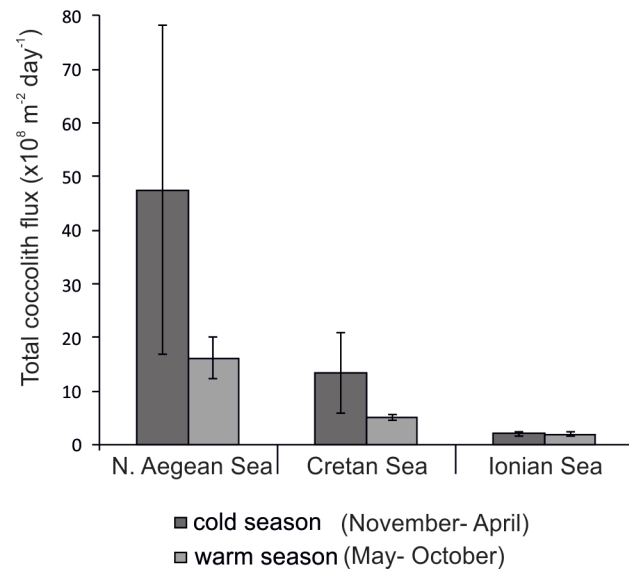


b) Cretan Sea



c) Ionian Sea





NATIONAL AND KAPODISTRIAN UNIVERSITY OF ATHENS
SCHOOL OF SCIENCES
FACULTY OF GEOLOGY & GEOENVIRONMENT
DEPARTMENT OF HISTORICAL GEOLOGY-PALAEONTOLOGY

Athens22/10/2019

Dear Editor

Herein I am submitting the revised manuscript entitled

" Coccolithophore export in three deep sea sites of the Aegean and Ionian Seas (Eastern Mediterranean): biogeographical patterns and biogenic carbonate fluxes "

by E. Skampa, M.V. Triantaphyllou, M.D. Dimiza, A. Gogou, E. Malinverno, S. Stavrakakis, C. Parinos, I.P.

Panagiotopoulos, D. Tselenti, O. Archontikis, K.-H. Baumann

in order to be published in Deep Sea Research II,

and I declare no conflict of interest.

Awaiting for your answer, I thank you in advance.

Sincerely

Prof. Maria Triantaphyllou

* Corresponding author